JOURNAL OF AERONAUTICAL MATERIALS
ISSN: 1005-5053
Vol. 43, Issue-01, 2023
pp. 1398-1436

USING THE VULNERABILITY INDEX FOR PERFORMANCE-BASED SEISMIC ASSESSMENT OF REINFORCED CONCRETE FRAMES AND CLEARLY ARTICULATING THE PERFORMANCE LEVELS

Abhay Hirekhan[1], Mohd. Zameeruddin[2] and Prabhakar S. Charpe[3]

[1]Research Scholar, Department of Civil Engineering, Kalinga University, New Raipur Chhattisgarh, 400 019, India; hir12312@rediffmail.com

[2]Associate Professor, Department of Civil Engineering, MGM's College of Engineering, Nanded. Maharashtra, 431 605, India; md_zameeruddin@mgmcen.ac.in
[3]Professor, Department of Civil Engineering, Kalinga University, New Raipur Chhattisgarh, 400 019, India; prabhakar.charpe@gmail.com

ABSTRACT

The majority of seismic design codes used today apply a "response reduction/ modification factor" to the structure's strength and serviceability parameters in order to account for a structure's inelastic behavior. By taking into consideration nonlinear behavior and deformation limitations, this factor enables a designer to apply Force-Based Design (FBD), a linear elastic process. However, when these structures were exposed to seismic forces, it was discovered that they were damaged or collapsed, thereby raises question towards the adequacy of FBD design methodology. Performance-based Seismic Design (PBSB) as on known today is capable to overcome these shortcomings and provides procedures to evaluate and assess the performance of the structural component or whole structural system for a given seismic hazard. These procedures provide information about nonlinear incursions in structural components, but they do not clearly scale the damage state of a structural component or whole structural system in a numeric number. In present study we have attempted to provide an empirical relationship between the damage state and performance level of a structural system. For this seventy-five 2D moment resisting bare frames have been designed following the guidelines of Indian seismic codes for FBD and their performance are evaluated using performance evaluation procedures described in PBSD. The possible integration of a damage states of these frames with respective building performance levels is proposed using engineering demand parameters resulted from nonlinear analysis. The approach provides a single step verification process that uses proposed vulnerability index, which reduces the iterative efforts in quantification or scaling of damage.

Keywords: Damage states, pushover analysis, engineering demand parameters, vulnerability Indices

INTRODUCTION

The increase in urbanization has led towards the vertical growth of residential and commercial structures. These structures when subjected to natural hazards such as Earthquakes, Hurricanes and Tornados sustained structural damages and claimed major life losses. In reinforced concrete structure (RC) ductility depends on the percentage of rebars and permissible limits in stress and strain for both concrete and steel, hence demands accurate modelling of structural components at local as well as global levels. Limit state design discussed in present seismic codes practice in India and its sub continents uses amplification factor for strength and ductility. Such an indirect approach misleads towards the quantification of nonlinear parameters [Zameeruddin and Sangle, 2016; Ghobarah, 2001]

In FBD approach, the reduced design force value is usually used. Some structures built in accordance with these design rules, whose primary goal is to preserve life, do withstand earthquakes, but it is impossible to efficiently reduce the direct and indirect economic losses brought on by major, much alone moderate, or mild earthquakes. The damages and losses frequently exceed the estimates of the designers, and these losses show that they will become more severe as the economy grows and population density rises. This has led researchers to realize that the old seismic codes have some limitations in terms of seismic concepts, meeting the demands of society, and various other areas [Ronald and Huburger, 2005] .

As awareness of the significance of inelastic structural response to large earthquakes grew in the 1960s and 1970s, the scientific community became more engaged in efforts to assess the inelastic deformation capacity of components of the structure. As a result, in order to address the shortcomings of FBD, first approaches have been developed to complement and enhance the already-existing FBD, eventually leading to the more practical approach that is founded on displacement consideration. One of the outcomes of these attempts is the performance-based seismic design (PBSD) that the Federal Emergency Management Agency (FEMA) has suggested. When a structure is designed using performance-based principles, nonlinear static and dynamic analyses are used to determine the structure's behavior and the acceptable degree of performance levels.

Pushover analysis (POA), a nonlinear static analysis, is used to identify and evaluate the building's capabilities in order to have a more precise seismic evaluation, which is thought of as a crucial step in the performance-based design procedure. PBSD makes it easier to design and build structures with a real and accurate assessment of the probability of physical and direct & indirect economic loss that may be experienced as a consequence of future seismic hazards (Al-Haddad and Siddiqui, 1995; Ghobarah, 2001). Due to this approach's uniqueness, it is regarded as one of the most reliable seismic design approaches. ATC 40 (1996), FEMA 273 (1996), FEMA 356 (2000), FEMA 440 (2005), ASCE 41 (2006), and FEMA 445 (2006) are just a few of the reference documents that were produced as a result of the emergence of PBSD methods.

Pushover Analysis

Nonlinear analysis approaches play a crucial role in the recently established performance-based seismic design procedure in determining the nature and degree of severity of damage, which are then used to evaluate a structure's inelastic behavior and understand the structure's failure modes during major earthquakes. Pushover analysis, which was detailed by the Applied Technology Council (ATC-40) and FEMA-356, is a simplified static nonlinear process wherein the structure is subjected to predetermined, monotonically increasing lateral forces until a plastic collapse mechanism is attained. It is based on mathematical modelling that takes into account the nonlinear behavior characteristics of each structural and non-structural component of the structure, which are evaluated by strength and deformation capacities.

The procedure usually follows a lumped-plasticity process, which checks the spread of inelasticity through the generation of nonlinear plastic hinges at both ends of the structural components during every step of the incremental loading process. Performance, capacity and demand are the three main components which need to be determined in nonlinear static analysis approach. Pushover analysis, which originated according to the frame's first mode response, assumes that the fundamental mode of vibration is the primary response of the frame. Push over curve is shown in Fig. 1.

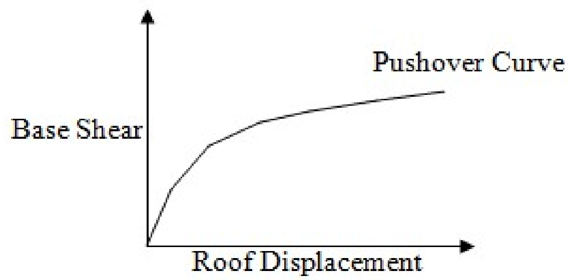

Fig. 1: Pushover curve

This analysis assesses the performance of the structure beyond its elastic limits when subjected to ground motion and this performance assessment includes the evaluation of structure's response parameters such as member forces, deformation, drift and inter storey drift. These parameters are considered as a predictor of damages of the structure and named as engineering demand parameters (EDPs). Based on the formation of plastic hinges during the collapse mechanism, these EDPs, which indicate the deformation capabilities of a structure, are used to define distinctive levels of damage and associated losses, that resulted from particular ground motion, in terms of different performance levels (Zameeruddin and Sangle, 2016; Ghobarah, 2001). These performance levels, such as immediate occupancy (IO), life safety (LS), and collapse prevention (CP), were defined by FEMA 356 (FEMA 356). Fig.2 shows performance level specified by FEMA 356.

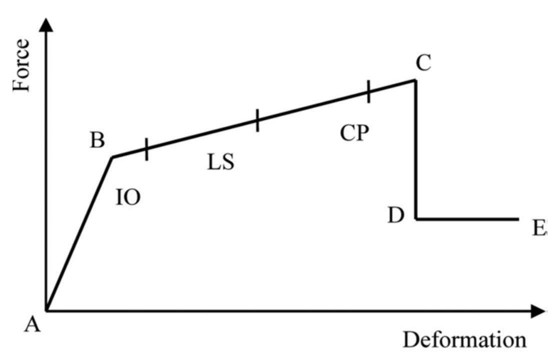

Fig. 2: Force-deformation Relationship of a Typical Plastic Hinge

Quantification of Damage

Damage to structural component initiates with the spalling of concrete cover, later extends to the concrete core. Cracking of concrete core is due to failure of concrete or steel. Concrete being a brittle component fails first, then steel yields [Ghorbah A., 1999; Zameeruddin and Sangle, 2017a]. In FBD structural component are design as primary tension members, hence the entire failure is governing by moment-rotation characteristics of steel. Under seismic loads inelastic excursion in steel appears which demand proper modeling of structural components. Various EDPs that are involved in damage mechanism includes a strain, a stress, a displacement or a rotation. Loss in any of these EDPs during inelastic phase may be term as loss in capacity. This loss in capacity may be identified as vulnerability. The scaling of these losses in the range of zero to one is called as vulnerability index [Suna et al., 2010; Apruba Mondal et al., 2013]. To understand the behavior of RC structures under inertia loads or seismic loads Pushover Analysis (POA) has been in extensive use. Due to its simple process, it has been common in practice.

PBSD has put forth various performance evaluation techniques using POA. These performance evaluation methods are capable to define plastic collapse mechanism of a structure at local and global levels. In addition, various structural and non-structural performance levels have been defined using the drift criterion. These performance levels are the acceptable risk of damage to the structure attained at a particular drift attainment under inertia loads or seismic loads. In its present state they are capable to identify a damage state, but are not capable to provide numeric damage scaling. In the present study some Vulnerability Indices (VI's) has been proposed to integrate the performance-based evaluation process with numeric assessment of damage using EDP's resulted from POA.

VI's are a dimensionless parameter that varies between 0 and 1 in a numeric scale. Zero represents an undamaged state of structure and 1 represent a fully damaged or collapsed state of structure, with intermediate values giving some measure of the degree of partial damage to the structure. In present study damage states of 75 2D-RCMRFs are evaluated using VI's calibrated from the EDPs resulted in POA. Figure 3, illustrates the procedure adopted for assessing a damage to structural component or overall structure. It's a continuation assessment process, which starts with the identification of collapse mechanism followed by the collection of EDPs associated with the identified damage state. Followed by preparation of correlation of structural performance levels with the damage state. The assessment ends with the quantification of a damage value in numeric scale.

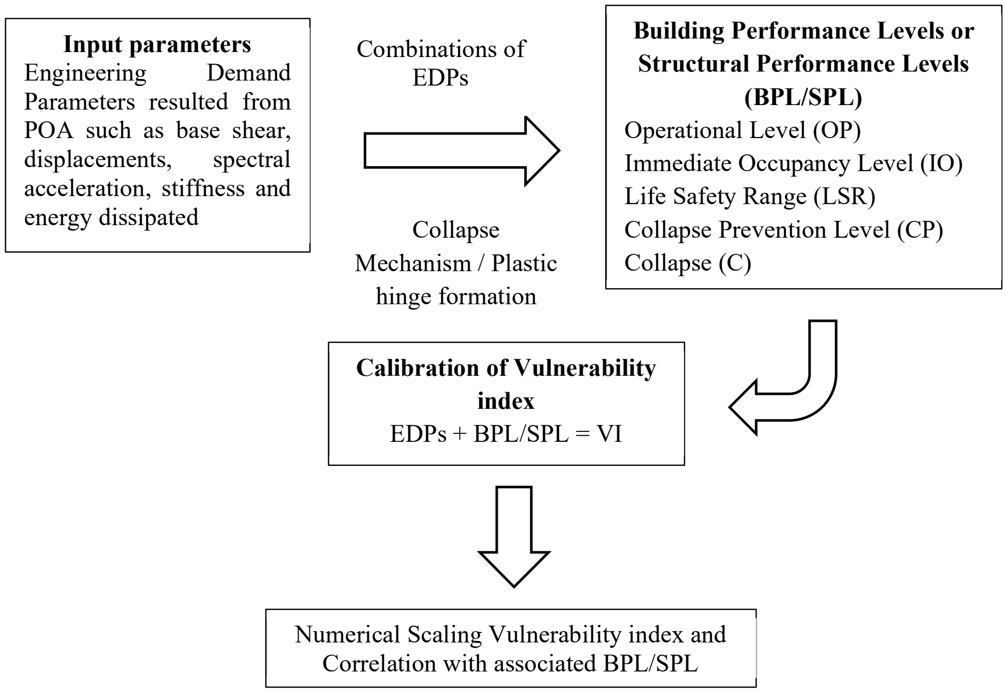

Fig. 3: Proposed Procedure of Vulnerability Index Assessment

PBSD has provided various performance evaluation procedures using POA. The output of POA describes the formation of plastic hinges and their transfer from one performance levels to other, stated as a collapse mechanism. The PBSD has defined various drift and rotation-based criterion for identification of attainment of a particular performance level, but do not provide numeric damage value, hence a vulnerability damage index is proposed herewith is used to answer a numeric damage value. The VI's attempts to correlate the damage state with identified performance levels using the associated EDPs resulting from POA. The EDPs used to form a VI's are base shear, displacements, stiffnesses and counts of plastic hinges formation in columns and beams.

The various assumptions made to identify a collapse mechanism and the associated plastic hinge formation are; (a) The first hinge formation at OP level either in beam or column is considered as elastic yield, (b) The first hinge formation in beam or column in IO, LS, CP are considered as attainment of elasto-plastic yield and (c) The first hinge formation in beam or column in C or E levels are considered as attainment of plastic yield. The proposed VI's are;

(i) Drift-based Vulnerability Index

The proposed vulnerability index is accounting the drift flow from elastic to plastic range at every discrete performance level. Mathematically expressed as;

$$VI_{drift} = \frac{d_j - d_{OP}}{d_{max} - d_{OP}} \quad \text{(i)}$$

Where in d_{OP} is the drift at the attainment of operational level, d_j is the drift of identified performance levels and d_{max} is the maximum overall drift attained by the system

(ii) Strength-based Vulnerability Index

The proposed vulnerability index is capable to quantify the loss in strength from elastic to plastic range at every discrete performance level. Mathematically expressed as;

$$VI_{Strength} = \frac{V_j - V_{OP}}{V_{max} - V_{OP}} \quad \text{(ii)}$$

Where in V_{OP} is the base shear at the attainment of operational level, V_j is the base shear of identified performance levels and V_{max} is the maximum base shear

(iii) Stiffness-based Vulnerability Index

The proposed vulnerability index is able to evaluate the loss in stiffness from elastic to plastic range at every at every discrete performance level. Mathematically expressed as;

$$VI_{Stiffness} = \frac{K_{OP} - K_J}{K_{OP} - K_U}$$

(iii)

Where in K_{OP} is the base shear at the attainment of operational level, K_j is the base shear of identified performance levels and K_u is the maximum base shear

(iv) Collapse mechanism-based Vulnerability Index

The proposed vulnerability index is able to assess the overall damage state on the basis of plastic hinge mechanism. The count of plastic hinges formed in beams and columns are used to evaluate the damage values for transit of plastic hinge from elastic to plastic range at every discrete performance level

$$VI_{PH} = \frac{PH_j}{PH_S} \quad \text{(iv)}$$

Where in PH_j is the count of plastic hinges formed in beams and columns in an identified performance level, PH_s is the count of plastic hinges assigned in beams and columns

Example RCMRFs

In this work, we assessed the seismic performance of reinforced concrete moment resisting frames (RCMRFs), which are representative of the basic building style used in India. For this analysis, 75 two dimensional RCMRFs with different numbers of storeys and bays that are put through displacement-controlled nonlinear static procedure (NLSP) are used. The aforementioned RCMRFs depict a typical office block in seismic zone V on soil of medium type, according to IS 1893 (2002). These RCMRFs consist of low, medium, and high-rise structures. Low-rise and high-rise buildings are defined as having a height that is less than or greater than to three times the length of their span of building, respectively. Buildings that fall in the middle are referred to as medium-rise buildings (Stafford and Coull, 1991).

According to the standards outlined in the succeeding generation of PBSE processes, the frame's response was assessed. The example structures' analytical modelling was done using SAP 2000V 17.0 (Wilson and Habibullah, 2000). While the storey width of RCMRFs varies from the first bay to the fifth bay, the story heights range from one to fifteen stories. Based on the number of bays, all 75 frames are grouped into five different groups. Group 1 includes 15 frames with one bay and different stories (1-15), Group 2 include 15 frames with two bays and different stories (1-15), Group 3 include 15 frames with three bays and different stories (1-15), Group 4 include 15 frames with four bays and different stories (1-15) and Group 5 include 15 frames with five bays and different stories (1-15). Table 1 lists the properties of these RCMRFs, and Fig. 5 shows how they are often laid out in practice.

The RCMRFs has a bay width of 3 m and a story height of 3 m. The RCMRFs are designed in accordance with the standards outlined in IS 456:2000 (Rev), and the provisions of IS 13920:1996 are used for detailing the RCMRFs' seismic ductility. According the guidelines of IS 1893:2002 (part 1), the frame was subjected to different pattern of lateral loads. Push1 represents trivial lateral load pattern as per IS 1893:2002, Push 2 represents the uniform lateral load pattern and Push 3 represents the elastic first mode lateral load pattern. Fig. 4 shows lateral distribution of load on example RCMRFs. P–Δ geometric nonlinearity effects were considered for each load combination used in this study. The design base shear for a building is derived as:

$$Vd = \frac{ZI\mathrm{Sa}}{2Rg}W$$

Where Z stands as a zone factor (Z = 0.36 for zone V), I stands as a structure's importance factor (I = 1 for these buildings), R stands as a response reduction factor (R = 5.0) for ductile or moment resisting frames (RCMRF), S_a stands as a spectral acceleration, and W stands as a structure's seismic weight. Fig. 3 shows lateral distribution of load on RCMRFs.

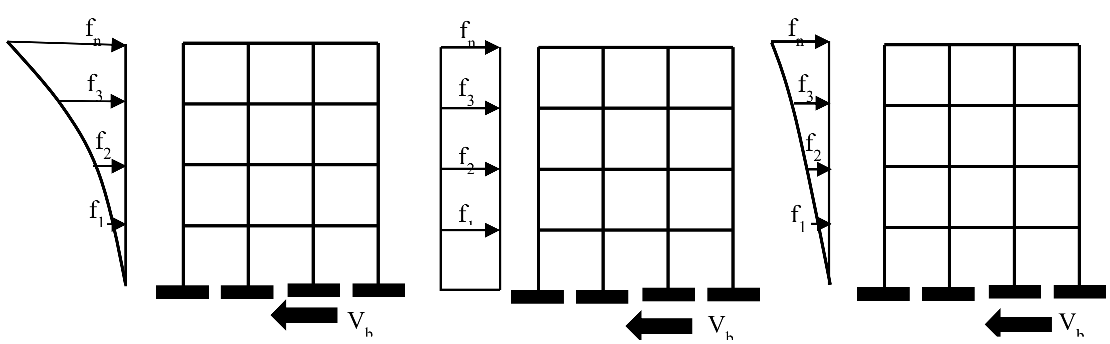

(a) IS 1893:2002 load pattern (Load case: Push 1)
(b) Uniform load pattern (Load case: Push 2)
(c) Elastic mode-1 pattern (Load case: Push 3)

Fig. 4: Shows lateral distribution of load on RCMRFs.

Table 1 Characteristics of the studied example RCMRFs

Group	MRFs	Stories	Column		Beam	
			Width (mm)	Depth (mm)	Width (mm)	Depth (mm)
1	S3B1	1 - 3	680	680	300	450
	S6B1	3 - 6	600	600	300	450
	S9B1	7 - 9	530	530	300	380
	S12B1	10 - 12	450	450	300	380
	S15B1	13 - 15	300	300	300	300
2	S3B2	1 - 3	680	680	300	450
	S6B2	3 - 6	600	600	300	450
	S9B2	7 - 9	530	530	300	380
	S12B2	10 - 12	450	450	300	380
	S15B2	13 - 15	300	300	300	300
3	S3B3	1 - 3	680	680	300	450
	S6B3	3 - 6	600	600	300	450
	S9B3	7 - 9	530	530	300	380
	S12B3	10 - 12	450	450	300	380
	S15B3	13 - 15	300	300	300	300
4	S3B4	1 - 3	680	680	300	450
	S6B4	3 - 6	600	600	300	450
	S9B4	7 - 9	530	530	300	380
	S12B4	10 - 12	450	450	300	380
	S15B4	13 - 15	300	300	300	300
5	S3B5	1 - 3	680	680	300	450
	S6B5	3 - 6	600	600	300	450
	S9B5	7 - 9	530	530	300	380
	S12B5	10 - 12	450	450	300	380
	S15B5	13 - 15	300	300	300	300

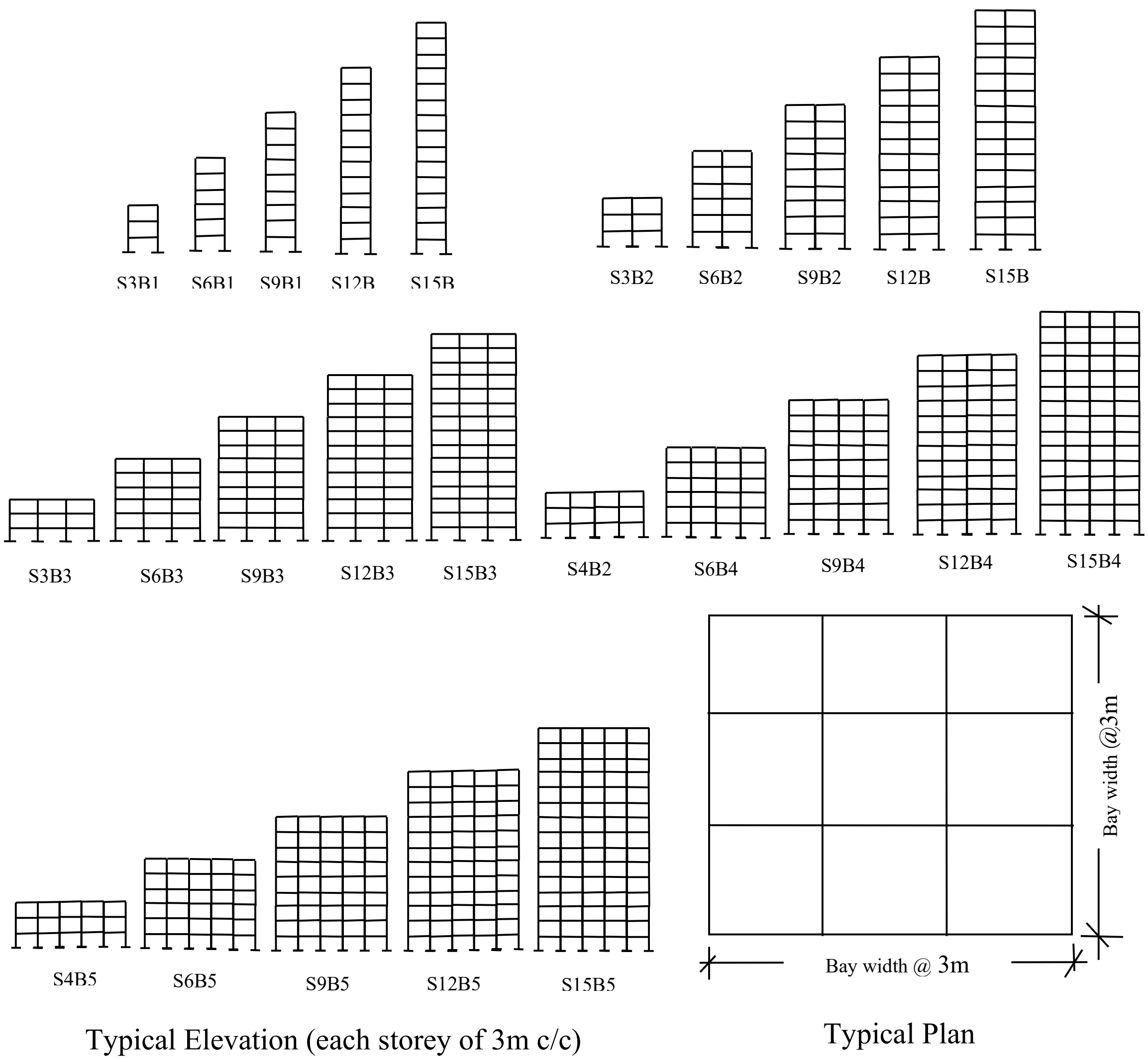

Fig. 5: Geometry and typical layout of studied RCMRFs.

For present example RCMRFs, seismic loads were calculated in accordance with IS 1893 - 2016 while dead and live loads were calculated in accordance with IS 875 - 1987 (Parts 1 and 2). A mean dead load of 18 KN/m (including finishes) and a mean live load of 4.5 KN/m, were assigned for each floor of example RCMRFs. The M25 grade concrete used in the RCMRFs has a 28-day characteristic cube strength of 25 MPa, and the Fe415 grade reinforcing steel used in the RCMRFs has a 500 MPa characteristic yield strength. Table 2 lists the material characteristics that were taken into account during design.

Table 2 Material Characteristics of RCMRFs

Material property of MRFs	Concrete Grade, M 25	Steel Grade, Fe 415
Weight per unit volume (KN/m^3)	25	76.97

Mass per unit volume (Kg/m^3)	2.548	7.849
Modulus of elasticity (KN/m^2)	25E+ 06	2E + 08
Characteristic strength (KN/m^2)	25000	45000 (yield)
Minimum tensile strength (KN/m^2)	-	485,800
Expected yield strength (KN/m^2)	-	465,500
Expected tensile strength(KN/m^2)	-	533,500

The example RCMRFs' structural design for demand estimation is not the only viable option. various designers may choose various answers to the same demand. The sizes of the RC members were chosen by according to a standard procedure used by engineers. For a planar frame, the cross section of the columns remained uniform in cross section up to three stories before it started to reduce, and the cross section of the beams did the same thing up to six stories before it started to reduce. Strong column-weak beam behavior is ensured by the RCMRF section design.

Modelling parameters and numerical acceptability standards along with the specifics of the lateral load profile and modal analysis are described in Table 3 and 4. A stress-strain relationship relating to FEMA 356-integrated software was utilized to construct a moment-rotation curve of a default plastic hinge. By placing concentrated M3 and P-M3 plastic hinges at both the ends of the beam and column, they were modelled as nonlinear frame components which has been shown in Fig. 6. The pushover curve derived from performance evaluation of an example RCMRF is illustrated in Fig. 7 (Ghobarah, 2000), along with the acceptance requirements for the maximum rotation capacity, denoted as immediate occupancy (IO), life safety (LS), and collapse prevention (CP).

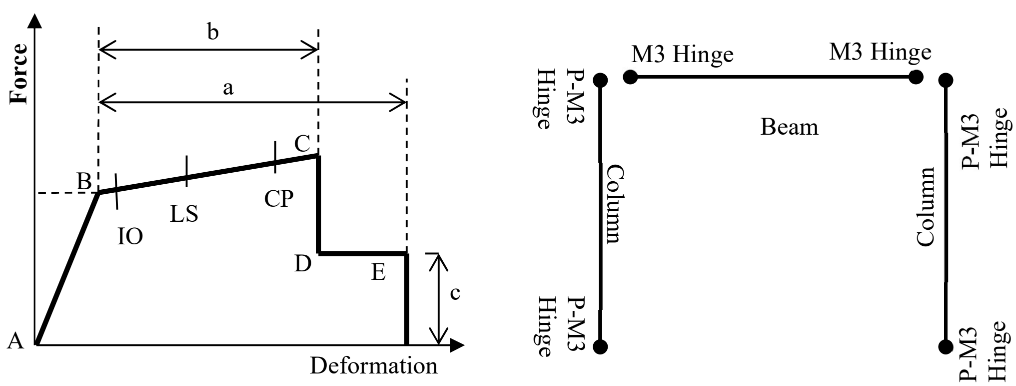

(a) Deformation control (flexure failure)   (b) Location of hinges

Fig. 6: Idealized inelastic force–deformation relationship

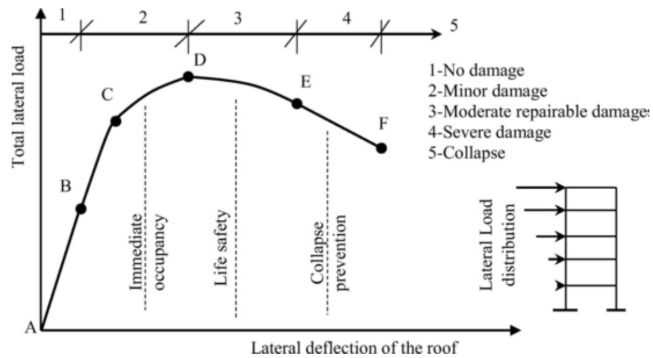

Fig. 7: Capacity curve representing pushover and associated damage states (Ghobarah, 2000).

Table 3: Modelling parameters and numerical acceptability standards for RC beams

Conditions			**Modeling Parameters**			**Acceptance Criteria**				
			Plastic rotation angle (radians)		Residual strength ratio	Plastic rotation angle (radians) Performance level				
$\frac{\rho-\rho'}{\rho_{bal}}$	Trans. Reinf.	$\frac{V}{b_w d\sqrt{f_c'}}$				IO	Component type			
							Primary		Secondary	
			A	B	c		LS	CP	LS	CP
≤ 0.0	C	≤ 3	0.025	0.05	0.2	0.010	0.020	0.025	0.02	0.05
≥ 0.5	C	≥ 3	0.020	0.03	0.2	0.005	0.010	0.02	0.02	0.03

Table 4: Modelling parameters and numerical acceptability standards for RC columns

Conditions			**Modeling Parameters**			**Acceptance Criteria**				
			Plastic rotation angle (radians)		Residual strength ratio	Plastic rotation angle (radians) Performance level				
$\frac{P}{A_g f_c'}$	Trans. Reinf.	$\frac{V}{b_w d\sqrt{f_c'}}$				IO	Component type			
							Primary		Secondary	
			A	B	c		LS	CP	LS	CP
≤ 0.1	C	≤ 3	0.02	0.03	0.2	0.005	0.015	0.02	0.02	0.03
≥ 0.40	C	≥ 3	0.015	0.025	0.2	0.003	0.012	0.015	0.0 18	0.025

Performance Assessment

In this study, we performed displacement-controlled NLSP on the example RCMRFs by using SAP 2000 V 17.0 (Wilson and Habibullah, 2000). The target displacement used for each RCMRF was 4% of the height of the frame (ATC 40, 1996). The analysis was conducted in two stages for the following: (i) gravity loads and (ii) predominant lateral loads.

In Stage I, gravity loads were applied as the distributed element loads on the basis of the yield line theory and concentrated loads from secondary beams. Gravity analysis was performed for full gravity load in a single step (i.e., force-control). The state of the structure in this analysis was saved and was subsequently recalled in Stage II.

In Stage II, lateral loads were applied monotonically in a step by- step nonlinear static analysis. Because the lateral force profile in pushover analysis influences the structural response, a set of lateral load patterns was used.

Results and discussions

PBSE procedures documented in PBSD is based on the damage state of a structure at local and global levels, that is structural performance levels and building performance levels. In its present form they are described in discrete performance level such as OP, IO, LS, CP and C. These performance levels are described in terms of attainment of permissible drift value. Such classifications are not directly understood by stakeholders Viz.; Contractor, Owner, Businessman and Government as they are having lack of seismic engineering knowledge. Hence, it's become necessary to communicate these performance levels in a language which is understandable by stakeholders. Table 5 provides the reconstructed performance levels names in its simple form. The present study intends to integrate a damage state with building performance levels, for this EDPs found from POA are used to identify the damage state and VI's has been defined. The introduced VI's includes (a) Drift -based VI, (b) Strength-based VI, (c) Stiffness-based VI and (d) Collapse mechanism-based VI.

Group of 75 2-D RCMRFs representing the general trend of construction in India and its sub-continents were modelled and analyzed. These groups represent low-rise, medium-rise and high-rise structures. Table 7 - 11 provides the values of proposed VI's for all such groups of RCMRFs. In POA incremental lateral loads are applied up to a targeted displacement. The distribution of these lateral loads along the height of structures plays an important role in collapse mechanism. In literature it has been suggested to use two set of lateral loads to obtain upper and lower bound values. That's way in present work we have adopted different push load cases. From the performance evaluation of all example RCMRFs it has been found that Push 1 load case gives lower bound values, Push 2 load case provides upper bound values and Push 3 results in median values [Hirekhan A., Zameeruddin M., Charpe P.S., 2023].

The non-linear modeling of RCMRFs depends on the position of plastic hinges assigned at columns and beams. In literature it has been suggested that for deformation-controlled (pure flexure) plastic hinges shall be at mid span of structural members. Whereas in force-controlled (pure shear) plastic hinges shall be at the ends of the structural members. In present study we have assigned plastic hinges at 10% and 90 % of the span to trace shear-flexure effects [Zameeruddin M., Sangle K.K., 2017a; Zameeruddin M., Sangle K.K., 2017b].

In PBSE procedures defined in CSM and DCM performance of structures is evaluated at performance point in terms of base shear and displacement values wherein no account of collapse mechanism in terms of formation of plastic hinges is taken care off. When the PBSE procedures were compared with each other significant difference was identified [Hirekhan A., Zameeruddin M., Charpe P.S.,2023]. With an intention to have complete check over the inelastic incursion different VI's as put forth.

The proposed drift-based VI traces the changes in ductility at every incremental step of POA, thus overcome the limitation of POA. Table 7 -11 provides the proposed VI values for all example RCMRFs. The envelope of response curve plotted between drift-based VI values and permissible drift limits provides a collapse zone. The trend lines for every response curve is capable to provide the damage values at any instantaneous displacement. Thus, it may be used for collapse zone identification for optimization of design of structural components. The increase in drift-based VI values is associated with the damages to structural components, that's why they may be related to associated repair.

The proposed strength-based VI provides the loss of strength at every incremental step of POA. This also overcomes the limitation of PBSE procedure to account for fall in strength in contrast to use the base shear at performance point. This help to utilize the reserve strength at other limit states, thereby structural design optimization can be done. Strength-based VI may be related to downtime of the structure as strengthening of structural member is needed to be done.

The proposed stiffness-based VI shows the fall in stiffness value at every incremental step. In present seismic code it has been referred as redundancy factor. The proposed stiffness-based VI may be used to trace the loss in stiffness at various performance levels and associated damages to frames and bays, thus it may be referred for assessment of casualties.

The collapse-mechanism based VI traces the fall of plastic hinges from one performance level to other and is associated with loss in strength and stiffness at every incremental step hence they may be related to repairs, downtime and casualties. The aim of the study was to integrate the proposed VI with PBSE. The present work forms a rational approach but for complete justification a set of groups of RCMRFs are needed to be analyzed, this has been kept as scope for further studies.

Table 5: Permissible drift limits at various performance levels and associated damage states (FEMA 356, 2000; ATC 40, 1996)

Performance level	Description	Drift limits
Operational Level (OP)	Structure does not undergo any damage	$< 0.7\%$
Immediate occupancy Level (IO)	Structural elements are partially damaged	1%

Life safety Level (LS)	Structural and non-structural elements of remarkable damage	2%
Collapse prevention Level (CP)	Structure is about to collapse	3%
Collapse Level (C)	Collapse	4%

In POA, collapse mechanism is represented through the formation of plastic hinges in columns & beams. The proposed vulnerability index has been defined in terms of attainment of various limit state of structural components associated with plastic hinge characteristics. The fall of plastic hinges from one performance level to other is tracked through the collapse mechanism. Formation of first plastic hinge considered as attainment of Operational level. Consecutive fall of plastic hinges in different limits of drift are identified to attain performance level is OP, IO, LS. CP. Table 6 shows possible way of integrating damage state with performance levels.

Table 6: Proposed relationship between VI's and performance levels

Performance level	Description	VI's Numeric Scale	Damage States
Operational Level (OP)	Structure does not undergo any damage	0	Ready for use
Immediate occupancy Level (IO)	Structural elements are partially damaged	0.10 - 0.25	Needed Repairs and Maintenance
Life safety Level (LS)	Structural and non-structural elements of remarkable damage	0.26 - 0.74	Not Ready to Use/Downtime
Collapse prevention Level (CP)	Structure is about to collapse	0.75 - 0.90	Causalities
Collapse Level (C)	Collapse	0.91 - 1.0	Major Causalities

An effort has been made to trace the EDPs responsible for performance of structural system in different limit state, in reference to attainment of various drift limits.

Table 7: VI's of Group I (One Bay) RCMRFs at discrete performance levels

Frame	**PL**	**Drift-Based VI**			**Strength-Based VI**			**Stiffness-Based VI**			**Collapse-Based VI**		
		Push 1	**Push 2**	**Push 3**	**Push 1**	**Push 2**	**Push 3**	**Push 1**	**Push 2**	**Push 3**	**Push 1**	**Push 2**	**Push 3**

S1B1	OP	0.000	0.000	0.000	0.000	0.000	0.000	0.000	0.000	0.000	0.000	0.000	0.000
	IO	0.013	0.013	0.013	0.294	0.298	0.287	0.000	0.000	0.000	0.167	0.167	0.167
	LS	0.329	0.329	0.328	0.911	0.911	0.911	0.878	0.877	0.878	0.667	0.667	0.667
	CP	1.000	1.000	1.000	1.000	1.000	1.000	1.000	1.000	1.000	0.667	0.667	0.667
	C	1.000	1.000	1.000	1.000	1.000	1.000	1.000	1.000	1.000	0.667	0.667	0.667
S2B1	OP	0.000	0.000	0.000	0.000	0.000	0.000	0.000	0.000	0.000	0.000	0.000	0.000
	IO	0.015	0.014	0.014	0.280	0.274	0.263	0.000	0.000	0.000	0.083	0.083	0.083
	LS	0.361	0.337	0.345	0.939	0.926	0.926	0.879	0.870	0.869	0.500	0.500	0.500
	CP	1.000	1.000	1.000	1.000	1.000	1.000	1.000	1.000	1.000	0.500	0.500	0.500
	C	1.000	1.000	1.000	1.000	1.000	1.000	1.000	1.000	1.000	0.500	0.500	0.500
S3B1	OP	0.000	0.000	0.000	0.000	0.000	0.000	0.000	0.000	0.000	0.000	0.000	0.000
	IO	0.013	0.001	0.014	0.227	0.016	0.240	0.000	0.000	0.000	0.056	0.056	0.056
	LS	0.395	0.363	0.388	0.942	0.957	0.943	0.885	0.864	0.883	0.444	0.444	0.444
	CP	1.000	1.000	1.000	1.000	1.000	1.000	1.000	0.959	1.000	0.444	0.444	0.444
	C	1.000	1.000	1.000	1.000	1.000	1.000	1.000	1.000	1.000	0.444	0.444	0.444
S4B1	OP	0.000	0.000	0.000	0.000	0.000	0.000	0.000	0.000	0.000	0.000	0.000	0.000
	IO	0.013	0.013	0.013	0.216	0.235	0.215	0.000	0.000	0.000	0.042	0.042	0.042
	LS	0.384	0.387	0.388	0.955	0.950	0.953	0.872	0.888	0.878	0.417	0.417	0.417
	CP	1.000	1.000	1.000	1.000	1.000	1.000	1.000	1.000	1.000	0.417	0.417	0.417
	C	1.000	1.000	1.000	1.000	1.000	1.000	1.000	1.000	1.000	0.417	0.417	0.417
S5B1	OP	0.000	0.000	0.000	0.000	0.000	0.000	0.000	0.000	0.000	0.000	0.000	0.000

	IO	0.014	0.011	0.013	0.225	0.206	0.212	0.000	0.000	0.000	0.033	0.033	0.033
	LS	0.392	0.395	0.387	0.967	0.965	0.963	0.873	0.887	0.874	0.400	0.400	0.400
	CP	1.000	1.000	1.000	1.000	1.000	1.000	1.000	1.000	1.000	0.400	0.400	0.400
	C	1.000	1.000	1.000	1.000	1.000	1.000	1.000	1.000	1.000	0.400	0.400	0.400
S6B1	OP	0.000	0.000	0.000	0.000	0.000	0.000	0.000	0.000	0.000	0.000	0.000	0.000
	IO	0.015	0.011	0.014	0.231	0.199	0.223	0.000	0.000	0.000	0.028	0.028	0.056
	LS	0.369	0.398	0.389	0.975	0.974	0.975	0.853	0.885	0.871	0.389	0.389	0.389
	CP	1.000	1.000	1.000	1.000	1.000	1.000	1.000	1.000	1.000	0.389	0.389	0.389
	C	1.000	1.000	1.000	1.000	1.000	1.000	1.000	1.000	1.000	0.389	0.389	0.389
S7B1	OP	0.000	0.000	0.000	0.000	0.000	0.000	0.000	0.000	0.000	0.000	0.000	0.000
	IO	0.017	0.012	0.015	0.251	0.209	0.234	0.000	0.000	0.000	0.024	0.024	0.024
	LS	0.366	0.392	0.371	0.973	0.989	0.990	0.848	0.879	0.854	0.357	0.381	0.381
	CP	1.000	1.000	1.000	1.000	1.000	1.000	1.000	1.000	1.000	0.357	0.381	0.381
	C	1.000	1.000	1.000	1.000	1.000	1.000	1.000	1.000	1.000	0.405	0.381	0.405
S8B1	OP	0.000	0.000	0.000	0.000	0.000	0.000	0.000	0.000	0.000	0.000	0.000	0.000
	IO	0.020	0.014	0.017	0.284	0.229	0.257	0.000	0.000	0.000	0.021	0.021	0.021
	LS	0.380	0.388	0.366	0.917	1.000	0.967	0.859	0.872	0.848	0.354	0.375	0.354
	CP	1.000	1.000	1.000	1.000	1.000	1.000	1.000	1.000	1.000	0.354	0.375	0.354
	C	1.000	1.000	1.000	1.000	1.000	1.000	1.000	1.000	1.000	0.396	0.375	0.396
S9B1	OP	0.000	0.000	0.000	0.000	0.000	0.000	0.000	0.000	0.000	0.000	0.000	0.000
	IO	0.001	0.016	0.021	0.026	0.186	0.289	0.000	0.000	0.000	0.037	0.037	0.019

	LS	0.378	0.384	0.379	0.813	0.745	0.925	0.866	0.865	0.856	0.333	0.370	0.352
	CP	1.000	0.979	1.000	1.000	0.745	1.000	1.000	1.000	1.000	0.333	0.370	0.352
	C	1.000	0.979	1.000	1.000	0.745	1.000	1.000	1.000	1.000	0.389	0.370	0.389
S10 B1	OP	0.000	0.000	0.000	0.000	0.000	0.000	0.000	0.000	0.000	0.000	0.000	0.000
	IO	0.005	0.018	0.002	0.081	0.262	0.035	0.000	0.000	0.000	0.017	0.017	0.033
	LS	0.384	0.361	0.349	0.765	1.000	0.837	0.866	0.835	0.846	0.333	0.367	0.333
	CP	1.000	1.000	1.000	1.000	1.000	1.000	1.000	1.000	1.000	0.333	0.367	0.333
	C	1.000	1.000	1.000	1.000	1.000	1.000	1.000	1.000	1.000	0.383	0.383	0.383
S11 B1	OP	0.000	0.000	0.000	0.000	0.000	0.000	0.000	0.000	0.000	0.000	0.000	0.000
	IO	0.007	0.021	0.006	0.121	0.285	0.091	0.000	0.000	0.000	0.015	0.015	0.015
	LS	0.377	0.366	0.356	0.871	1.000	0.804	0.844	0.828	0.839	0.333	0.318	0.333
	CP	1.000	1.000	1.000	1.192	1.000	1.000	0.988	1.000	1.000	0.394	0.318	0.333
	C	1.000	1.000	1.000	1.000	1.000	1.000	1.000	1.000	1.000	0.394	0.379	0.379
S12 B1	OP	0.000	0.000	0.000	0.000	0.000	0.000	0.000	0.000	0.000	0.000	0.000	0.000
	IO	0.008	0.025	0.009	0.104	0.305	0.119	0.000	0.000	0.000	0.014	0.014	0.014
	LS	0.392	0.382	0.360	0.742	0.966	0.747	0.851	0.833	0.838	0.319	0.319	0.306
	CP	1.000	1.000	1.000	1.000	1.000	1.000	1.000	1.000	1.000	0.319	0.319	0.306
	C	1.000	1.000	1.000	1.000	1.000	1.000	1.000	1.000	1.000	0.361	0.375	0.375
S13 B1	OP	0.000	0.000	0.000	0.000	0.000	0.000	0.000	0.000	0.000	0.000	0.000	0.000
	IO	0.011	0.003	0.011	0.137	0.052	0.131	0.000	0.000	0.000	0.013	0.013	0.013
	LS	0.393	0.340	0.364	0.739	0.873	0.719	0.837	0.815	0.835	0.308	0.295	0.308

	CP	1.000	1.000	1.000	1.000	1.000	1.000	0.986	1.000	1.000	0.359	0.295	0.308
	C	1.000	1.000	1.000	1.000	1.000	1.000	1.000	1.000	1.000	0.359	0.372	0.359
S14B1	OP	0.000	0.000	0.000	0.000	0.000	0.000	0.000	0.000	0.000	0.000	0.000	0.000
	IO	0.016	0.008	0.015	0.186	0.109	0.172	0.000	0.000	0.000	0.024	0.024	0.024
	LS	0.383	0.376	0.384	0.745	0.878	0.731	0.828	0.828	0.825	0.298	0.298	0.298
	CP	1.000	1.000	1.000	1.000	1.000	1.000	0.992	1.000	0.985	0.345	0.298	0.357
	C	1.000	1.000	1.000	1.000	1.000	1.000	1.000	1.000	1.000	0.345	0.345	0.357
S15B1	OP	0.000	0.000	0.000	0.000	0.000	0.000	0.000	0.000	0.000	0.000	0.000	0.000
	IO	0.023	0.013	0.022	0.243	0.167	0.231	0.000	0.000	0.000	0.011	0.011	0.022
	LS	0.420	0.407	0.390	0.779	0.839	0.757	0.827	0.839	0.819	0.300	0.278	0.289
	CP	1.000	1.000	1.000	1.000	1.000	1.000	0.992	1.000	0.991	0.333	0.278	0.322
	C	1.000	1.000	1.000	1.000	1.000	1.000	1.000	1.000	1.000	0.333	0.333	0.322

Table 8: VI's of Group II (Two Bay) RCMRFs at discrete performance levels

Frame	**PL**	**Drift-Based VI**			**Strength-Based VI**			**Stiffness-Based VI**			**Collapse-Based VI**		
		Push 1	**Push 2**	**Push 3**	**Push 1**	**Push 2**	**Push 3**	**Push 1**	**Push 2**	**Push 3**	**Push 1**	**Push 2**	**Push 3**
S1B2	OP	0.000	0.000	0.000	0.000	0.000	0.000	0.000	0.000	0.000	0.000	0.000	0.000
	IO	0.014	0.014	0.014	0.333	0.337	0.327	0.000	0.000	0.000	0.100	0.100	0.100
	LS	0.329	0.329	0.329	0.910	0.911	0.910	0.880	0.880	0.880	0.700	0.700	0.700
	CP	1.000	1.000	1.000	1.000	1.000	1.000	1.000	1.000	1.000	0.700	0.700	0.700
	C	1.000	1.000	1.000	1.000	1.000	1.000	1.000	1.000	1.000	0.700	0.700	0.700

S2B2	OP	0.000	0.000	0.000	0.000	0.000	0.000	0.000	0.000	0.000	0.000	0.000	0.000
	IO	0.017	0.017	0.017	0.329	0.348	0.338	0.000	0.000	0.000	0.050	0.050	0.100
	LS	0.349	0.338	0.345	0.925	0.924	0.924	0.876	0.875	0.876	0.550	0.550	0.550
	CP	1.000	1.000	1.000	1.000	1.000	1.000	1.000	1.000	1.000	0.550	0.550	0.550
	C	1.000	1.000	1.000	1.000	1.000	1.000	1.000	1.000	1.000	0.550	0.550	0.550
S3B2	OP	0.000	0.000	0.000	0.000	0.000	0.000	0.000	0.000	0.000	0.000	0.000	0.000
	IO	0.013	0.013	0.014	0.244	0.277	0.261	0.000	0.000	0.000	0.033	0.033	0.033
	LS	0.391	0.354	0.380	0.945	0.939	0.943	0.891	0.883	0.888	0.500	0.500	0.500
	CP	1.000	1.000	1.000	1.000	1.000	1.000	1.000	1.000	1.000	0.500	0.500	0.500
	C	1.000	1.000	1.000	1.000	1.000	1.000	1.000	1.000	1.000	0.500	0.500	0.500
S4B2	OP	0.000	0.000	0.000	0.000	0.000	0.000	0.000	0.000	0.000	0.000	0.000	0.000
	IO	0.012	0.012	0.011	0.215	0.233	0.213	0.000	0.000	0.000	0.025	0.025	0.025
	LS	0.395	0.376	0.394	0.956	0.953	0.956	0.888	0.890	0.892	0.475	0.475	0.475
	CP	1.000	1.000	1.000	1.000	1.000	1.000	1.000	1.000	1.000	0.475	0.475	0.475
	C	1.000	1.000	1.000	1.000	1.000	1.000	1.000	1.000	1.000	0.475	0.475	0.475
S5B2	OP	0.000	0.000	0.000	0.000	0.000	0.000	0.000	0.000	0.000	0.000	0.000	0.000
	IO	0.012	0.009	0.011	0.212	0.189	0.195	0.000	0.000	0.000	0.020	0.020	0.020
	LS	0.381	0.395	0.412	0.967	0.966	0.966	0.879	0.896	0.897	0.460	0.460	0.460
	CP	1.000	1.000	1.000	1.000	1.000	1.000	1.000	1.000	1.000	0.460	0.460	0.460
	C	1.000	1.000	1.000	1.000	1.000	1.000	1.000	1.000	1.000	0.380	0.460	0.460
S6B2	OP	0.000	0.000	0.000	0.000	0.000	0.000	0.000	0.000	0.000	0.000	0.000	0.000

	IO	0.013	0.009	0.012	0.211	0.173	0.202	0.000	0.000	0.000	0.017	0.017	0.033
	LS	0.371	0.386	0.378	0.976	0.976	0.976	0.864	0.882	0.872	0.450	0.450	0.450
	CP	1.000	1.000	1.000	1.000	1.000	1.000	1.000	1.000	1.000	0.450	0.450	0.450
	C	1.000	1.000	1.000	1.000	1.000	1.000	1.000	1.000	1.000	0.450	0.450	0.450
S7B2	OP	0.000	0.000	0.000	0.000	0.000	0.000	0.000	0.000	0.000	0.000	0.000	0.000
	IO	0.013	0.009	0.011	0.219	0.169	0.199	0.000	0.000	0.000	0.013	0.025	0.013
	LS	0.361	0.366	0.377	0.991	0.990	0.988	0.861	0.877	0.876	0.413	0.438	0.438
	CP	1.000	1.000	1.000	1.000	1.000	1.000	1.000	1.000	1.000	0.413	0.438	0.438
	C	1.000	1.000	1.000	1.000	1.000	1.000	1.000	1.000	1.000	0.450	0.438	0.450
S8B2	OP	0.000	0.000	0.000	0.000	0.000	0.000	0.000	0.000	0.000	0.000	0.000	0.000
	IO	0.015	0.015	0.012	0.244	0.296	0.211	0.000	0.000	0.000	0.013	0.025	0.013
	LS	0.364	0.348	0.361	0.929	0.918	1.000	0.867	0.874	0.862	0.413	0.438	0.438
	CP	1.000	1.001	1.000	1.000	1.000	1.000	1.000	0.995	1.000	0.413	0.438	0.438
	C	1.000	1.000	1.000	1.000	1.000	1.000	1.000	1.000	1.000	0.450	0.438	0.450
S9B2	OP	0.000	0.000	0.000	0.000	0.000	0.000	0.000	0.000	0.000	0.000	0.000	0.000
	IO	0.017	0.010	0.014	0.268	0.137	0.235	0.000	0.000	0.000	0.022	0.022	0.011
	LS	0.382	0.359	0.356	0.892	0.705	0.952	0.876	0.867	0.860	0.411	0.433	0.411
	CP	1.000	0.978	1.000	1.000	0.705	1.000	1.000	1.000	1.000	0.411	0.433	0.411
	C	1.000	0.978	1.000	1.000	0.705	1.000	1.000	1.000	1.000	0.444	0.433	0.444
S10B2	OP	0.000	0.000	0.000	0.000	0.000	0.000	0.000	0.000	0.000	0.000	0.000	0.000
	IO	0.019	0.011	0.016	0.269	0.192	0.248	0.000	0.000	0.000	0.020	0.020	0.020

	LS	0.385	0.365	0.346	0.853	1.000	0.915	0.874	0.857	0.851	0.400	0.410	0.410
	CP	1.000	1.000	1.000	1.000	1.000	1.000	1.000	1.000	1.000	0.400	0.410	0.410
	C	1.000	1.000	1.000	1.000	1.000	1.000	1.000	1.000	1.000	0.440	0.440	0.440
S11 B2	OP	0.000	0.000	0.000	0.000	0.000	0.000	0.000	0.000	0.000	0.000	0.000	0.000
	IO	0.019	0.014	0.019	0.243	0.220	0.278	0.000	0.000	0.000	0.009	0.009	0.018
	LS	0.379	0.354	0.344	0.822	0.991	0.859	0.864	0.844	0.849	0.373	0.373	0.373
	CP	1.000	1.000	1.000	1.000	1.000	1.000	1.000	1.000	1.000	0.373	0.373	0.373
	C	1.000	1.000	1.000	1.000	1.000	1.000	1.000	1.000	1.000	0.445	0.436	0.436
S12 B2	OP	0.000	0.000	0.000	0.000	0.000	0.000	0.000	0.000	0.000	0.000	0.000	0.000
	IO	0.020	0.016	0.020	0.228	0.236	0.247	0.000	0.000	0.000	0.008	0.008	0.008
	LS	0.367	0.356	0.380	0.776	0.916	0.816	0.854	0.842	0.863	0.367	0.350	0.358
	CP	1.000	1.000	1.000	1.000	1.000	1.000	1.000	1.000	1.000	0.367	0.350	0.358
	C	1.000	1.000	1.000	1.000	1.000	1.000	1.000	1.000	1.000	0.425	0.417	0.433
S13 B2	OP	0.000	0.000	0.000	0.000	0.000	0.000	0.000	0.000	0.000	0.000	0.000	0.000
	IO	0.021	0.018	0.021	0.235	0.258	0.234	0.000	0.000	0.000	0.008	0.008	0.008
	LS	0.418	0.393	0.365	0.822	0.939	0.773	0.868	0.858	0.849	0.369	0.400	0.308
	CP	1.000	1.000	1.000	1.000	1.000	1.000	0.996	1.000	1.000	0.415	0.400	0.308
	C	1.000	1.000	1.000	1.000	1.000	1.000	1.000	1.000	1.000	0.415	0.408	0.431
S14 B2	OP	0.000	0.000	0.000	0.000	0.000	0.000	0.000	0.000	0.000	0.000	0.000	0.000
	IO	0.023	0.022	0.023	0.250	0.483	0.252	0.000	0.000	0.000	0.007	0.007	0.014
	LS	0.392	0.489	0.380	0.824	0.985	0.814	0.840	0.891	0.839	0.350	0.350	0.350

	CP	1.000	1.000	1.000	1.000	1.000	1.000	0.992	1.000	0.996	0.386	0.350	0.393
	C	1.000	1.000	1.000	1.000	1.000	1.000	1.000	1.000	1.000	0.386	0.386	0.393
S15B2	OP	0.000	0.000	0.000	0.000	0.000	0.000	0.000	0.000	0.000	0.000	0.000	0.000
	IO	0.027	0.026	0.026	0.279	0.307	0.273	0.000	0.000	0.000	0.007	0.013	0.007
	LS	0.412	0.376	0.404	0.860	0.880	0.852	0.838	0.834	0.840	0.353	0.313	0.353
	CP	1.000	1.000	1.000	1.000	1.000	1.000	0.991	1.000	0.995	0.387	0.313	0.380
	C	1.000	1.000	1.000	1.000	1.000	1.000	1.000	1.000	1.000	0.387	0.380	0.380

Table 9: VI's of Group III (Three Bay) RCMRFs at discrete performance levels

Frame	**PL**	**Drift-Based VI**			**Strength-Based VI**			**Stiffness-Based VI**			**Collapse-Based VI**		
		Push 1	**Push 2**	**Push 3**	**Push 1**	**Push 2**	**Push 3**	**Push 1**	**Push 2**	**Push 3**	**Push 1**	**Push 2**	**Push 3**
S1B3	OP	0.000	0.000	0.000	0.000	0.000	0.000	0.000	0.000	0.000	0.000	0.000	0.000
	IO	0.014	0.014	0.014	0.335	0.339	0.329	0.000	0.000	0.000	0.071	0.071	0.071
	LS	0.329	0.329	0.329	0.911	0.911	0.911	0.881	0.881	0.881	0.714	0.714	0.714
	CP	1.000	1.000	1.000	1.000	1.000	1.000	1.000	1.000	1.000	0.714	0.714	0.714
	C	1.000	1.000	1.000	1.000	1.000	1.000	1.000	1.000	1.000	0.714	0.714	0.714
S2B3	OP	0.000	0.000	0.000	0.000	0.000	0.000	0.000	0.000	0.000	0.000	0.000	0.000
	IO	0.018	0.007	0.015	0.224	0.095	0.192	0.000	0.000	0.000	0.036	0.036	0.036
	LS	0.277	0.249	0.264	0.884	0.879	0.881	0.688	0.663	0.674	0.500	0.500	0.500
	CP	1.000	1.000	1.000	1.000	1.000	1.000	1.000	1.000	1.000	0.500	0.500	0.500
	C	1.000	1.000	1.000	1.000	1.000	1.000	1.000	1.000	1.000	0.571	0.607	0.571

	OP	0.000	0.000	0.000	0.000	0.000	0.000	0.000	0.000	0.000	0.000	0.000	0.000
	IO	0.013	0.013	0.014	0.259	0.274	0.278	0.000	0.000	0.000	0.024	0.024	0.024
S3B3	LS	0.388	0.348	0.376	0.945	0.938	0.943	0.893	0.884	0.890	0.524	0.524	0.524
	CP	1.000	1.000	1.000	1.000	1.000	1.000	1.000	1.000	1.000	0.524	0.524	0.524
	C	1.000	1.000	1.000	1.000	1.000	1.000	1.000	1.000	1.000	0.524	0.524	0.524
	OP	0.000	0.000	0.000	0.000	0.000	0.000	0.000	0.000	0.000	0.000	0.000	0.000
	IO	0.012	0.012	0.011	0.223	0.242	0.220	0.000	0.000	0.000	0.018	0.018	0.018
S4B3	LS	0.390	0.371	0.412	0.956	0.953	0.957	0.890	0.891	0.902	0.500	0.500	0.500
	CP	1.000	1.000	1.000	1.000	1.000	1.000	1.000	1.000	1.000	0.500	0.500	0.500
	C	1.000	1.000	1.000	1.000	1.000	1.000	1.000	1.000	1.000	0.500	0.500	0.500
	OP	0.000	0.000	0.000	0.000	0.000	0.000	0.000	0.000	0.000	0.000	0.000	0.000
	IO	0.012	0.009	0.010	0.218	0.192	0.198	0.000	0.000	0.000	0.014	0.014	0.014
S5B3	LS	0.377	0.408	0.384	0.967	0.967	0.967	0.881	0.903	0.888	0.486	0.486	0.486
	CP	1.000	1.000	1.000	1.000	1.000	1.000	1.000	1.000	1.000	0.486	0.486	0.486
	C	1.000	1.000	1.000	1.000	1.000	1.000	1.000	1.000	1.000	0.486	0.486	0.486
	OP	0.000	0.000	0.000	0.000	0.000	0.000	0.000	0.000	0.000	0.000	0.000	0.000
	IO	0.012	0.008	0.010	0.216	0.169	0.196	0.000	0.000	0.000	0.012	0.012	0.012
S6B3	LS	0.380	0.373	0.375	0.978	0.978	0.977	0.881	0.885	0.881	0.476	0.476	0.476
	CP	1.000	1.000	1.000	1.000	1.000	1.000	1.000	1.000	1.000	0.476	0.476	0.476
	C	1.000	1.000	1.000	1.000	1.000	1.000	1.000	1.000	1.000	0.476	0.476	0.476
S7B3	OP	0.000	0.000	0.000	0.000	0.000	0.000	0.000	0.000	0.000	0.000	0.000	0.000

	IO	0.012	0.008	0.010	0.230	0.170	0.207	0.000	0.000	0.000	0.010	0.010	0.010
	LS	0.390	0.367	0.380	0.992	0.989	0.989	0.886	0.884	0.886	0.469	0.469	0.469
	CP	1.000	1.000	1.000	1.000	1.000	1.000	1.000	1.000	1.000	0.469	0.469	0.469
	C	1.000	1.000	1.000	1.000	1.000	1.000	1.000	1.000	1.000	0.480	0.469	0.480
S8B3	OP	0.000	0.000	0.000	0.000	0.000	0.000	0.000	0.000	0.000	0.000	0.000	0.000
	IO	0.014	0.008	0.008	0.248	0.174	0.212	0.000	0.000	0.000	0.009	0.009	0.009
	LS	0.370	0.350	0.385	0.950	1.000	1.000	0.876	0.869	0.882	0.438	0.464	0.473
	CP	1.000	1.000	1.000	1.000	1.000	1.000	1.000	1.000	1.000	0.438	0.464	0.473
	C	1.000	1.000	1.000	1.000	1.000	1.000	1.000	1.000	1.000	0.473	0.464	0.473
S9B3	OP	0.000	0.000	0.000	0.000	0.000	0.000	0.000	0.000	0.000	0.000	0.000	0.000
	IO	0.016	0.009	0.013	0.276	0.128	0.234	0.000	0.000	0.000	0.008	0.016	0.008
	LS	0.367	0.323	0.343	0.898	0.688	0.963	0.876	0.852	0.859	0.437	0.437	0.437
	CP	1.000	0.978	1.000	1.000	0.688	1.000	1.000	1.000	1.000	0.437	0.437	0.437
	C	1.000	0.978	1.000	1.000	0.688	1.000	1.000	1.000	1.000	0.468	0.460	0.468
S10B3	OP	0.000	0.000	0.000	0.000	0.000	0.000	0.000	0.000	0.000	0.000	0.000	0.000
	IO	0.018	0.011	0.015	0.291	0.201	0.257	0.000	0.000	0.000	0.014	0.014	0.007
	LS	0.356	0.332	0.337	0.862	1.000	0.928	0.866	0.844	0.854	0.429	0.414	0.407
	CP	1.000	1.000	1.000	1.000	1.000	1.000	1.000	1.000	1.000	0.429	0.414	0.407
	C	1.000	1.000	1.000	1.000	1.000	1.000	1.000	1.000	1.000	0.464	0.464	0.464
S11B3	OP	0.000	0.000	0.000	0.000	0.000	0.000	0.000	0.000	0.000	0.000	0.000	0.000
	IO	0.017	0.012	0.018	0.241	0.212	0.279	0.000	0.000	0.000	0.006	0.006	0.013

	LS	0.385	0.356	0.351	0.827	0.982	0.865	0.874	0.851	0.861	0.403	0.377	0.390
	CP	1.000	1.000	1.000	1.000	1.000	1.000	1.000	1.000	1.000	0.403	0.377	0.390
	C	1.000	1.000	1.000	1.000	1.000	1.000	1.000	1.000	1.000	0.468	0.461	0.461
S12 B3	OP	0.000	0.000	0.000	0.000	0.000	0.000	0.000	0.000	0.000	0.000	0.000	0.000
	IO	0.017	0.014	0.017	0.219	0.228	0.242	0.000	0.000	0.000	0.006	0.006	0.006
	LS	0.408	0.368	0.400	0.794	0.937	0.833	0.873	0.857	0.880	0.393	0.363	0.387
	CP	1.006	1.000	1.000	1.000	1.000	1.000	0.991	1.000	1.000	0.393	0.363	0.387
	C	1.000	1.000	1.000	1.000	1.000	1.000	1.000	1.000	1.000	0.446	0.435	0.458
S13 B3	OP	0.000	0.000	0.000	0.000	0.000	0.000	0.000	0.000	0.000	0.000	0.000	0.000
	IO	0.018	0.016	0.018	0.226	0.249	0.224	0.000	0.000	0.000	0.011	0.005	0.005
	LS	0.374	0.389	0.418	0.802	0.936	0.801	0.856	0.865	0.883	0.374	0.352	0.374
	CP	1.000	1.000	1.000	1.000	1.000	1.000	1.000	1.000	1.000	0.374	0.352	0.374
	C	1.000	1.000	1.000	1.000	1.000	1.000	1.000	1.000	1.000	0.440	0.423	0.440
S14 B3	OP	0.000	0.000	0.000	0.000	0.000	0.000	0.000	0.000	0.000	0.000	0.000	0.000
	IO	0.020	0.019	0.020	0.239	0.276	0.242	0.000	0.000	0.000	0.005	0.005	0.010
	LS	0.384	0.359	0.373	0.833	0.902	0.822	0.843	0.846	0.846	0.378	0.342	0.362
	CP	1.000	1.000	1.000	1.000	1.000	1.000	0.990	1.000	1.000	0.413	0.342	0.362
	C	1.000	1.000	1.000	1.000	1.000	1.000	1.000	1.000	1.000	0.413	0.403	0.408
S15 B3	OP	0.000	0.000	0.000	0.000	0.000	0.000	0.000	0.000	0.000	0.000	0.000	0.000
	IO	0.023	0.022	0.022	0.266	0.294	0.259	0.000	0.000	0.000	0.005	0.005	0.005
	LS	0.410	0.385	0.379	0.873	0.892	0.856	0.849	0.850	0.832	0.381	0.005	0.357

	CP	1.000	1.000	1.001	1.000	1.000	1.000	0.994	1.000	0.994	0.400	0.329	0.405
	C	1.000	1.000	1.000	1.000	1.000	1.000	1.000	1.000	1.000	0.400	0.405	0.405

Table 10: VI's of Group IV (Four Bay) RCMRFs at discrete performance levels

Frame	**PL**	**Drift-Based VI**			**Strength-Based VI**			**Stiffness-Based VI**			**Collapse-Based VI**		
		Push 1	**Push 2**	**Push 3**	**Push 1**	**Push 2**	**Push 3**	**Push 1**	**Push 2**	**Push 3**	**Push 1**	**Push 2**	**Push 3**
S1B4	OP	0.000	0.000	0.000	0.000	0.000	0.000	0.000	0.000	0.000	0.000	0.000	0.000
	IO	0.014	0.014	0.018	0.337	0.341	0.445	0.000	0.000	0.000	0.056	0.056	0.111
	LS	0.329	0.329	0.328	0.911	0.911	0.901	0.882	0.881	0.885	0.722	0.722	0.722
	CP	1.000	1.000	1.000	1.000	1.000	1.000	1.000	1.000	1.000	0.722	0.722	0.722
	C	1.000	1.000	1.000	1.000	1.000	1.000	1.000	1.000	1.000	0.722	0.722	0.722
S2B4	OP	0.000	0.000	0.000	0.000	0.000	0.000	0.000	0.000	0.000	0.000	0.000	0.000
	IO	0.014	0.014	0.014	0.292	0.301	0.292	0.000	0.000	0.000	0.028	0.028	0.028
	LS	0.343	0.332	0.340	0.926	0.924	0.927	0.878	0.878	0.878	0.583	0.583	0.583
	CP	1.000	1.000	1.000	1.000	1.000	1.000	1.000	1.000	1.000	0.583	0.583	0.583
	C	1.000	1.000	1.000	1.000	1.000	1.000	1.000	1.000	1.000	0.583	0.583	0.583
S3B4	OP	0.000	0.000	0.000	0.000	0.000	0.000	0.000	0.000	0.000	0.000	0.000	0.000
	IO	0.014	0.012	0.014	0.268	0.272	0.288	0.000	0.000	0.000	0.019	0.019	0.019
	LS	0.387	0.346	0.374	0.943	0.937	0.943	0.894	0.884	0.891	0.537	0.537	0.537
	CP	1.000	1.000	1.000	1.000	1.000	1.000	1.000	1.000	1.000	0.537	0.537	0.537
	C	1.000	1.000	1.000	1.000	1.000	1.000	1.000	1.000	1.000	0.537	0.537	0.537

S4B4	OP	0.000	0.000	0.000	0.000	0.000	0.000	0.000	0.000	0.000	0.000	0.000	0.000
	IO	0.012	0.011	0.011	0.227	0.247	0.225	0.000	0.000	0.000	0.014	0.014	0.014
	LS	0.387	0.386	0.410	0.955	0.954	0.957	0.891	0.899	0.902	0.514	0.514	0.514
	CP	1.000	1.000	1.000	1.000	1.000	1.000	1.000	1.000	1.000	0.514	0.514	0.514
	C	1.000	1.000	1.000	1.000	1.000	1.000	1.000	1.000	1.000	0.514	0.514	0.514
S5B4	OP	0.000	0.000	0.000	0.000	0.000	0.000	0.000	0.000	0.000	0.000	0.000	0.000
	IO	0.012	0.009	0.010	0.222	0.195	0.201	0.000	0.000	0.000	0.011	0.011	0.011
	LS	0.391	0.406	0.402	0.968	0.967	0.968	0.890	0.904	0.897	0.500	0.500	0.500
	CP	1.000	1.000	1.000	1.000	1.000	1.000	1.000	1.000	1.000	0.500	0.500	0.500
	C	1.000	1.000	1.000	1.000	1.000	1.000	1.000	1.000	1.000	0.500	0.500	0.500
S6B4	OP	0.000	0.000	0.000	0.000	0.000	0.000	0.000	0.000	0.000	0.000	0.000	0.000
	IO	0.012	0.008	0.010	0.222	0.169	0.197	0.000	0.000	0.000	0.009	0.009	0.009
	LS	0.375	0.369	0.392	0.977	0.977	0.979	0.881	0.885	0.890	0.491	0.491	0.491
	CP	1.000	1.000	1.000	1.000	1.000	1.000	1.000	1.000	1.000	0.491	0.491	0.491
	C	1.000	1.000	1.000	1.000	1.000	1.000	1.000	1.000	1.000	0.491	0.491	0.491
S7B4	OP	0.000	0.000	0.000	0.000	0.000	0.000	0.000	0.000	0.000	0.000	0.000	0.000
	IO	0.012	0.008	0.010	0.230	0.165	0.206	0.000	0.000	0.000	0.008	0.008	0.016
	LS	0.363	0.380	0.395	0.990	0.991	0.991	0.873	0.889	0.893	0.484	0.151	0.484
	CP	1.000	1.000	1.000	1.000	1.000	1.000	1.000	1.000	1.000	0.484	0.151	0.484
	C	1.000	1.000	1.000	1.000	1.000	1.000	1.000	1.000	1.000	0.492	0.484	0.484
S8B4	OP	0.000	0.000	0.000	0.000	0.000	0.000	0.000	0.000	0.000	0.000	0.000	0.000

	IO	0.014	0.008	0.011	0.254	0.172	0.215	0.000	0.000	0.000	0.007	0.007	0.007
	LS	0.359	0.359	0.354	0.948	1.000	1.000	0.873	0.875	0.868	0.451	0.479	0.479
	CP	1.000	1.000	1.000	1.000	1.000	1.000	1.000	1.000	1.000	0.451	0.479	0.479
	C	1.000	1.000	1.000	1.000	1.000	1.000	1.000	1.000	1.000	0.486	0.479	0.486
S9B4	OP	0.000	0.000	0.000	0.000	0.000	0.000	0.000	0.000	0.000	0.000	0.000	0.000
	IO	0.016	0.009	0.012	0.283	0.125	0.237	0.000	0.000	0.000	0.012	0.006	0.006
	LS	0.377	0.361	0.355	0.911	0.679	0.986	0.882	0.876	0.867	0.451	0.451	0.451
	CP	1.000	0.977	1.000	1.000	0.679	1.000	1.000	1.000	1.000	0.451	0.451	0.451
	C	1.000	0.977	1.000	1.000	0.679	1.000	1.000	1.000	1.000	0.481	0.475	0.481
S10B4	OP	0.000	0.000	0.000	0.000	0.000	0.000	0.000	0.000	0.000	0.000	0.000	0.000
	IO	0.019	0.010	0.015	0.301	0.201	0.260	0.000	0.000	0.000	0.011	0.011	0.006
	LS	0.379	0.374	0.340	0.880	1.000	0.930	0.848	0.873	0.858	0.450	0.428	0.422
	CP	1.030	1.000	1.000	1.000	1.000	1.000	0.969	1.000	1.000	0.478	0.428	0.422
	C	1.000	1.000	1.000	1.000	1.000	1.000	1.000	1.000	1.000	0.478	0.478	0.478
S11B4	OP	0.000	0.000	0.000	0.000	0.000	0.000	0.000	0.000	0.000	0.000	0.000	0.000
	IO	0.017	0.012	0.017	0.250	0.212	0.286	0.000	0.000	0.000	0.005	0.010	0.010
	LS	0.382	0.360	0.380	0.828	0.978	0.889	0.877	0.856	0.878	0.404	0.389	0.404
	CP	1.000	1.000	1.000	1.000	1.000	1.000	1.000	1.000	1.000	0.404	0.389	0.404
	C	1.000	1.000	1.000	1.000	1.000	1.000	1.000	1.000	1.000	0.480	0.475	0.475
S12B4	OP	0.000	0.000	0.000	0.000	0.000	0.000	0.000	0.000	0.000	0.000	0.000	0.000
	IO	0.017	0.014	0.017	0.224	0.229	0.250	0.000	0.000	0.000	0.005	0.005	0.005

	LS	0.378	0.358	0.386	0.777	0.935	0.821	0.873	0.857	0.879	0.403	0.375	0.384
	CP	1.000	1.000	1.000	1.000	1.000	1.000	1.000	1.000	1.000	0.403	0.375	0.384
	C	1.000	1.000	1.000	1.000	1.000	1.000	1.000	1.000	1.000	0.449	0.435	0.477
S13 B4	OP	0.000	0.000	0.000	0.000	0.000	0.000	0.000	0.000	0.000	0.000	0.000	0.000
	IO	0.018	0.016	0.018	0.234	0.248	0.231	0.000	0.000	0.000	0.009	0.004	0.004
	LS	0.372	0.383	0.401	0.800	0.926	0.792	0.859	0.866	0.878	0.389	0.359	0.380
	CP	1.000	1.000	1.000	1.000	1.000	1.000	1.000	1.000	1.000	0.389	0.359	0.380
	C	1.000	1.000	1.000	1.000	1.000	1.000	1.000	1.000	1.000	0.453	0.436	0.444
S14 B4	OP	0.000	0.000	0.000	0.000	0.000	0.000	0.000	0.000	0.000	0.000	0.000	0.000
	IO	0.020	0.018	0.020	0.250	0.278	0.251	0.000	0.000	0.000	0.004	0.004	0.008
	LS	0.369	0.390	0.397	0.836	0.925	0.835	0.835	0.866	0.865	0.393	0.349	0.377
	CP	1.000	1.000	1.000	1.000	1.000	1.000	0.987	1.000	1.000	0.393	0.349	0.377
	C	1.000	1.000	1.000	1.000	1.000	1.000	1.000	1.000	1.000	0.429	0.417	0.417
S15 B4	OP	0.000	0.000	0.000	0.000	0.000	0.000	0.000	0.000	0.000	0.000	0.000	0.000
	IO	0.023	0.022	0.022	0.278	0.305	0.270	0.000	0.000	0.000	0.004	0.007	0.004
	LS	0.409	0.380	0.393	0.880	0.892	0.866	0.857	0.852	0.839	0.396	0.337	0.367
	CP	1.000	1.000	1.000	1.000	1.000	1.000	1.000	1.000	0.986	0.396	0.337	0.415
	C	1.000	1.000	1.000	1.000	1.000	1.000	1.000	1.000	1.000	0.415	0.407	0.415

Table 11: VI's of Group V (Five Bay) RCMRFs at discrete performance levels

Frame	**PL**	**Drift-Based VI**	**Strength-Based VI**	**Stiffness-Based VI**	**Collapse-Based VI**

		Push 1	**Push 2**	**Push 3**	**Push 1**	**Push 2**	**Push 3**	**Push 1**	**Push 2**	**Push 3**	**Push 1**	**Push 2**	**Push 3**
S1B5	OP	0.000	0.000	0.000	0.000	0.000	0.000	0.000	0.000	0.000	0.000	0.000	0.000
	IO	0.018	0.018	0.018	0.326	0.328	0.321	0.000	0.000	0.000	0.045	0.045	0.045
	LS	0.341	0.341	0.341	0.925	0.925	0.925	0.865	0.864	0.864	0.727	0.727	0.727
	CP	1.000	1.000	1.000	1.000	1.000	1.000	1.000	1.000	1.000	0.727	0.727	0.727
	C	1.000	1.000	1.000	1.000	1.000	1.000	1.000	1.000	1.000	0.727	0.727	0.727
S2B5	OP	0.000	0.000	0.000	0.000	0.000	0.000	0.000	0.000	0.000	0.000	0.000	0.000
	IO	0.014	0.013	0.013	0.296	0.305	0.305	0.000	0.000	0.000	0.023	0.023	0.023
	LS	0.344	0.317	0.313	0.928	0.921	0.921	0.879	0.860	0.851	0.591	0.591	0.591
	CP	1.000	0.964	0.952	1.000	1.000	1.000	1.000	0.981	0.970	0.591	0.591	0.591
	C	1.000	1.000	1.000	1.000	1.000	1.000	1.000	1.000	1.000	0.591	0.591	0.591
S3B5	OP	0.000	0.000	0.000	0.000	0.000	0.000	0.000	0.000	0.000	0.000	0.000	0.000
	IO	0.014	0.012	0.014	0.275	0.271	0.294	0.000	0.000	0.000	0.015	0.015	0.030
	LS	0.386	0.345	0.372	0.945	0.938	0.943	0.895	0.884	0.891	0.545	0.545	0.545
	CP	1.000	1.000	1.000	1.000	1.000	1.000	1.000	1.000	1.000	0.545	0.545	0.545
	C	1.000	1.000	1.000	1.000	1.000	1.000	1.000	1.000	1.000	0.545	0.545	0.545
S4B5	OP	0.000	0.000	0.000	0.000	0.000	0.000	0.000	0.000	0.000	0.000	0.000	0.000
	IO	0.024	0.026	0.026	0.236	0.282	0.282	0.000	0.000	0.000	0.015	0.015	0.030
	LS	0.419	0.466	0.466	0.941	0.941	0.941	0.765	0.819	0.819	0.545	0.545	0.545
	CP	0.981	1.000	1.000	1.000	1.000	1.000	0.984	1.000	1.000	0.545	0.545	0.545
	C	1.000	1.000	1.000	1.000	1.000	1.000	1.000	1.000	1.000	0.545	0.545	0.545

S5B5	OP	0.000	0.000	0.000	0.000	0.000	0.000	0.000	0.000	0.000	0.000	0.000	0.000
	IO	0.011	0.009	0.010	0.225	0.197	0.203	0.000	0.000	0.000	0.009	0.009	0.009
	LS	0.384	0.371	0.389	0.962	0.966	0.967	0.889	0.891	0.894	0.509	0.509	0.509
	CP	1.000	1.000	1.000	1.000	1.000	1.000	1.000	1.000	1.000	0.509	0.509	0.509
	C	1.000	1.000	1.000	1.000	1.000	1.000	1.000	1.000	1.000	0.509	0.509	0.509
S6B5	OP	0.000	0.000	0.000	0.000	0.000	0.000	0.000	0.000	0.000	0.000	0.000	0.000
	IO	0.011	0.008	0.010	0.226	0.170	0.197	0.000	0.000	0.000	0.008	0.008	0.008
	LS	0.388	0.406	0.381	0.979	0.979	0.974	0.890	0.901	0.888	0.500	0.500	0.500
	CP	1.000	1.000	1.000	1.000	1.000	1.000	1.000	1.000	1.000	0.500	0.500	0.500
	C	1.000	1.000	1.000	1.000	1.000	1.000	1.000	1.000	1.000	0.500	0.500	0.500
S7B5	OP	0.000	0.000	0.000	0.000	0.000	0.000	0.000	0.000	0.000	0.000	0.000	0.000
	IO	0.012	0.008	0.010	0.233	0.165	0.209	0.000	0.000	0.000	0.006	0.006	0.013
	LS	0.359	0.352	0.369	0.988	0.991	0.990	0.872	0.876	0.882	0.500	0.494	0.494
	CP	1.000	1.000	1.000	1.000	1.000	1.000	1.000	1.000	1.000	0.500	0.494	0.494
	C	1.000	1.000	1.000	1.000	1.000	1.000	1.000	1.000	1.000	0.500	0.494	0.494
S8B5	OP	0.000	0.000	0.000	0.000	0.000	0.000	0.000	0.000	0.000	0.000	0.000	0.000
	IO	0.012	0.007	0.010	0.236	0.144	0.196	0.000	0.000	0.000	0.006	0.006	0.006
	LS	0.358	0.325	0.359	0.991	0.987	1.000	0.872	0.858	0.874	0.489	0.438	0.489
	CP	1.000	1.000	1.000	1.000	1.000	1.000	1.000	1.000	1.000	0.489	0.438	0.489
	C	1.000	1.000	1.000	1.000	1.000	1.000	1.000	1.000	1.000	0.494	0.489	0.494
S9B5	OP	0.000	0.000	0.000	0.000	0.000	0.000	0.000	0.000	0.000	0.000	0.000	0.000

	IO	0.016	0.009	0.012	0.288	0.124	0.239	0.000	0.000	0.000	0.010	0.005	0.005
	LS	0.364	0.351	0.345	0.910	0.673	0.984	0.878	0.871	0.863	0.460	0.455	0.460
	CP	1.000	0.977	1.000	1.000	0.673	1.000	1.000	1.000	1.000	0.460	0.455	0.460
	C	1.000	0.977	1.000	1.000	0.673	1.000	1.000	1.000	1.000	0.490	0.485	0.490
S10 B5	OP	0.000	0.000	0.000	0.000	0.000	0.000	0.000	0.000	0.000	0.000	0.000	0.000
	IO	0.018	0.010	0.014	0.308	0.201	0.263	0.000	0.000	0.000	0.009	0.009	0.005
	LS	0.355	0.331	0.328	0.879	0.995	0.925	0.871	0.850	0.855	0.459	0.441	0.427
	CP	1.000	1.000	1.000	1.000	1.000	1.000	1.000	1.000	1.000	0.459	0.441	0.427
	C	1.000	1.000	1.000	1.000	1.000	1.000	1.000	1.000	1.000	0.486	0.486	0.486
S11 B5	OP	0.000	0.000	0.000	0.000	0.000	0.000	0.000	0.000	0.000	0.000	0.000	0.000
	IO	0.017	0.009	0.015	0.273	0.172	0.250	0.000	0.000	0.000	0.004	0.004	0.004
	LS	0.354	0.375	0.352	0.840	0.983	0.890	0.870	0.868	0.864	0.413	0.397	0.393
	CP	1.000	1.000	1.000	1.000	1.000	1.000	1.000	1.000	1.000	0.413	0.397	0.393
	C	1.000	1.000	1.000	1.000	1.000	1.000	1.000	1.000	1.000	0.483	0.442	0.483
S12 B5	OP	0.000	0.000	0.000	0.000	0.000	0.000	0.000	0.000	0.000	0.000	0.000	0.000
	IO	0.017	0.013	0.017	0.229	0.232	0.258	0.000	0.000	0.000	0.004	0.004	0.004
	LS	0.394	0.370	0.381	0.784	0.952	0.819	0.882	0.864	0.878	0.413	0.383	0.394
	CP	1.000	1.000	1.000	1.000	1.000	1.000	1.000	1.000	1.000	0.413	0.383	0.394
	C	1.000	1.000	1.000	1.000	1.000	1.000	1.000	1.000	1.000	0.481	0.443	0.485
S13 B5	OP	0.000	0.000	0.000	0.000	0.000	0.000	0.000	0.000	0.000	0.000	0.000	0.000
	IO	0.018	0.015	0.018	0.241	0.251	0.238	0.000	0.000	0.000	0.007	0.003	0.003

	LS	0.393	0.372	0.367	0.810	0.925	0.779	0.872	0.864	0.865	0.399	0.367	0.381
	CP	1.000	1.000	1.000	1.000	1.000	1.000	1.000	1.000	1.000	0.399	0.367	0.381
	C	1.000	1.000	1.000	1.000	1.000	1.000	1.000	1.000	1.000	0.448	0.441	0.462
	OP	0.000	0.000	0.000	0.000	0.000	0.000	0.000	0.000	0.000	0.000	0.000	0.000
	IO	0.020	0.018	0.020	0.259	0.281	0.258	0.000	0.000	0.000	0.003	0.003	0.006
S14 B5	LS	0.386	0.376	0.387	0.845	0.920	0.833	0.859	0.862	0.862	0.403	0.357	0.380
	CP	1.000	1.000	1.000	1.000	1.000	1.000	1.000	1.000	1.000	0.403	0.357	0.380
	C	1.000	1.000	1.000	1.000	1.000	1.000	1.000	1.000	1.000	0.429	0.425	0.429
	OP	0.000	0.000	0.000	0.000	0.000	0.000	0.000	0.000	0.000	0.000	0.000	0.000
	IO	0.023	0.022	0.022	0.289	0.311	0.281	0.000	0.000	0.000	0.003	0.006	0.003
S15 B5	LS	0.388	0.398	0.375	0.880	0.906	0.865	0.846	0.864	0.839	0.406	0.348	0.376
	CP	1.000	1.000	1.002	1.000	1.000	1.000	1.000	1.000	0.997	0.406	0.348	0.376
	C	1.000	1.000	1.000	1.000	1.000	1.000	1.000	1.000	1.000	0.424	0.415	0.424

The VI's provides the damage state of the structure and follows the collapse mechanism yielded in various limit states. These VI's when compared with permissible drift limits provides the upper and lower bound response of structure during a seismic event. The grouping of example frames with increasing number of storeys and bays provides a damage envelope for category of building under selected case. These responses are useful to visualize the extend of damage and quantification of various collapse zone. Figure 8 (i) – (lxi) shows the damage spectrum group of RCMRFs in respect to defines VI's.

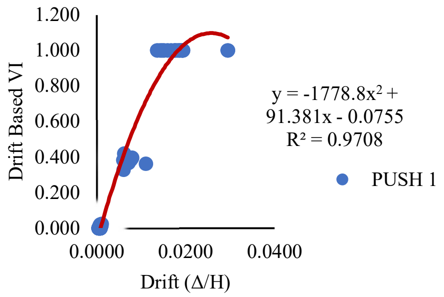

(i) Drift Based VI Group – 01

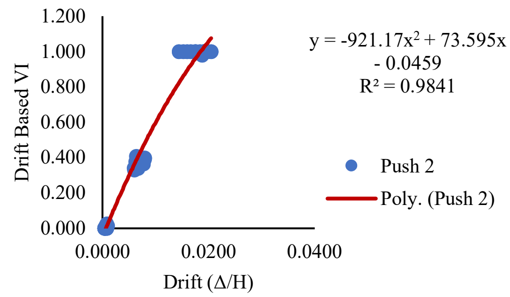

(ii) Drift Based VI Group – 01

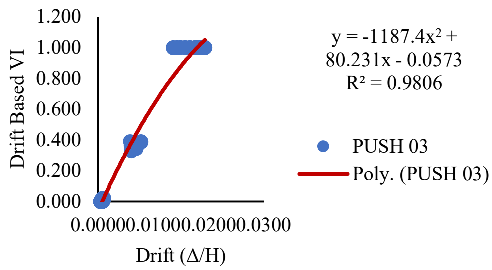

(iii) Drift Based VI Group – 01

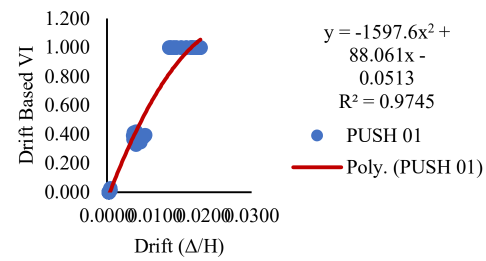

(iv) Drift Based VI Group – 02

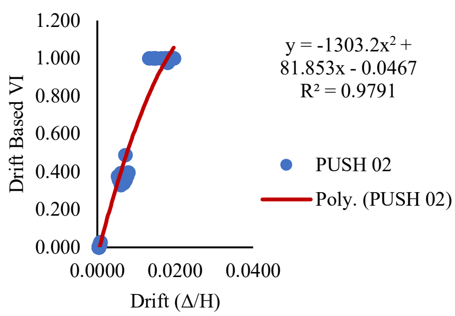

(v) Drift Based VI Group – 02

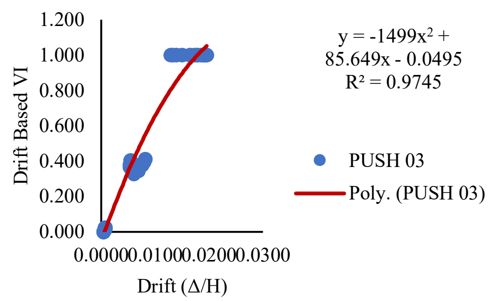

(vi) Drift Based VI Group – 02

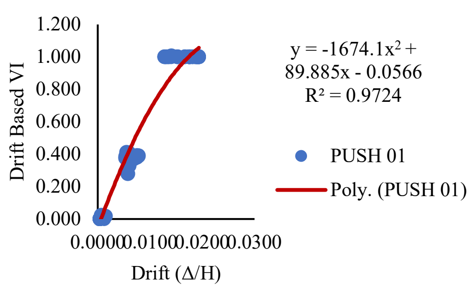

(vii) Drift Based VI Group – 03

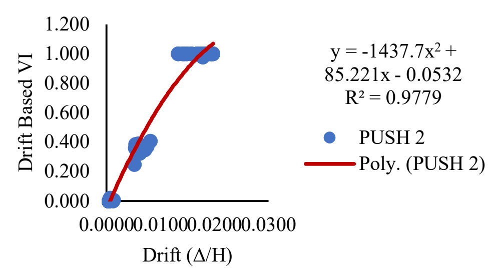

(viii) Drift Based VI Group – 03

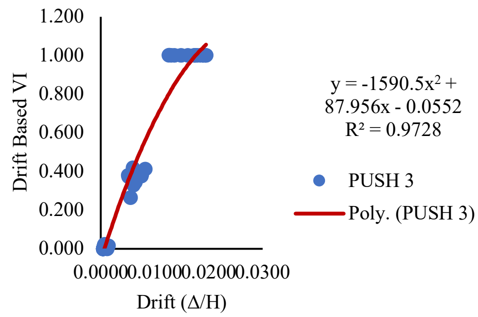

(ix) Drift Based VI Group – 03

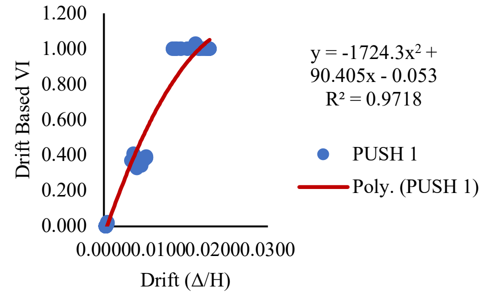

(x) Drift Based VI Group – 04

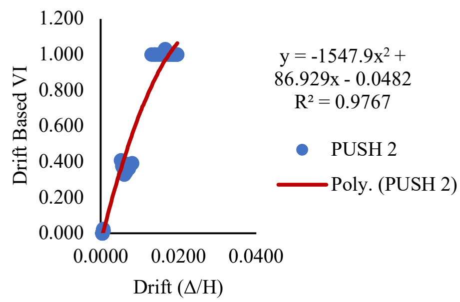

(xi) Drift Based VI Group – 04

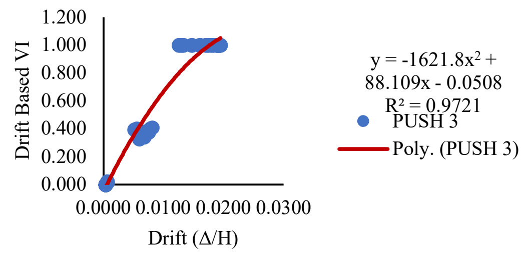

(xii) Drift Based VI Group – 04

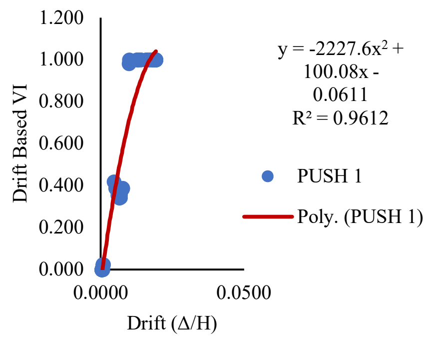

(xiii) Drift Based VI Group – 05

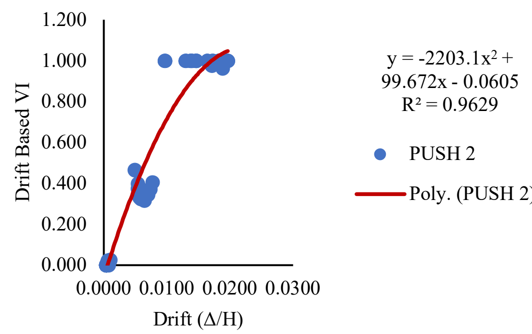

(xiv) Drift Based VI Group – 05

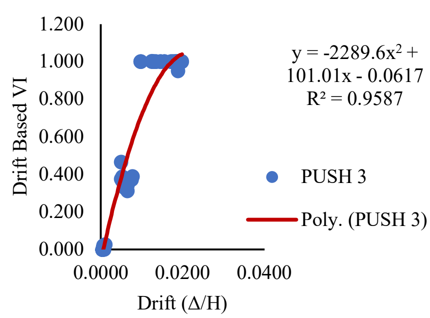

(xv) Drift Based VI Group – 05

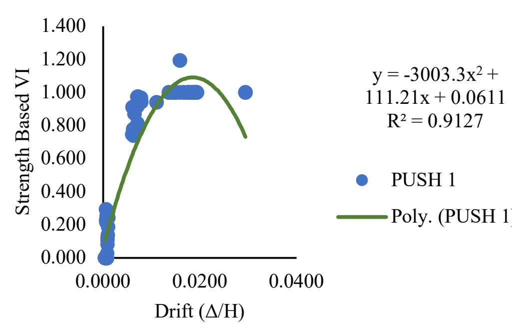

(xvi) Strength Based VI Group – 01

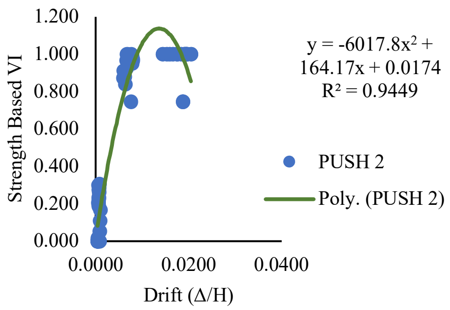

(xvii) Strength Based VI Group – 01

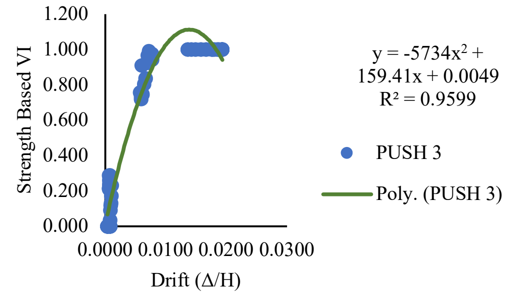

(xviii) Strength Based VI Group – 01

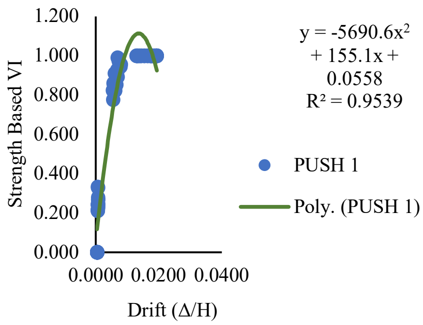

(xix) Strength Based VI Group – 02

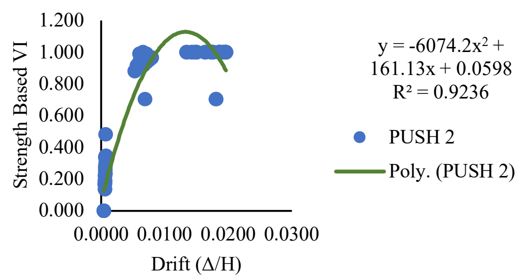

(xx) Strength Based VI Group – 02

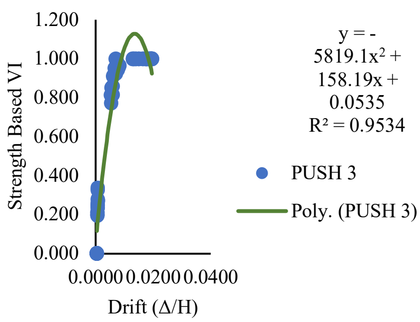

(xxi) Strength Based VI Group – 02

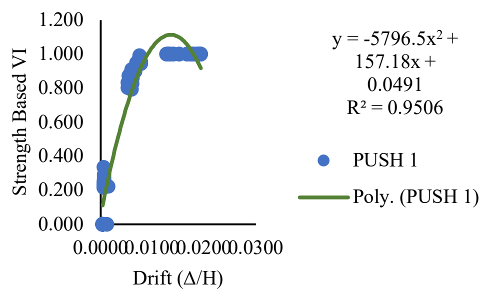

(xxii) Strength Based VI Group – 03

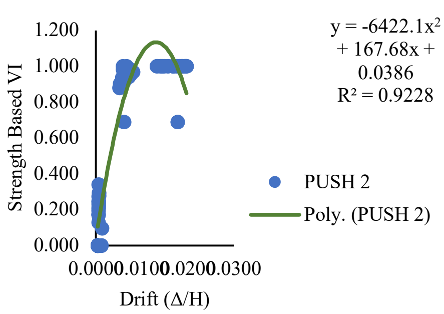

(xxiii) Strength Based VI Group – 03

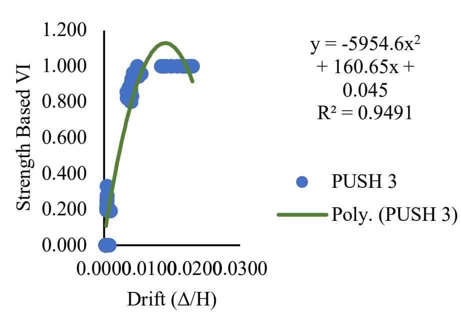

(xxiv) Strength Based VI Group – 03

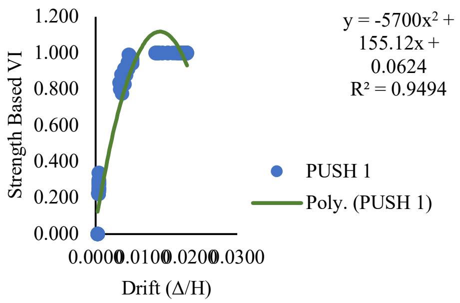

(xxv) Strength Based VI Group – 04

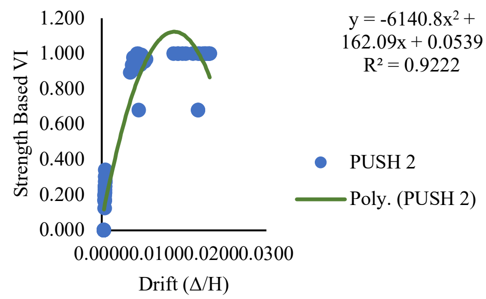

(xxvi) Strength Based VI Group – 04

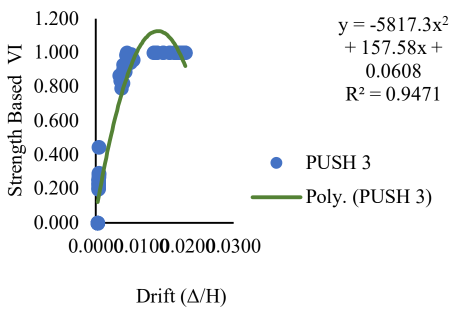

(xxvii) Strength Based VI Group – 04

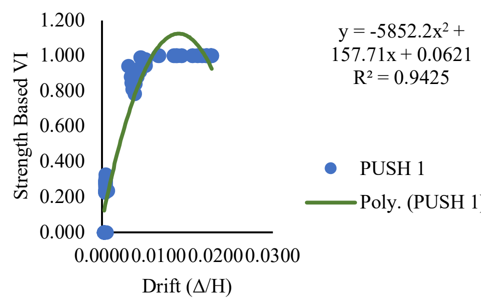

(xxviii) Strength Based VI Group – 05

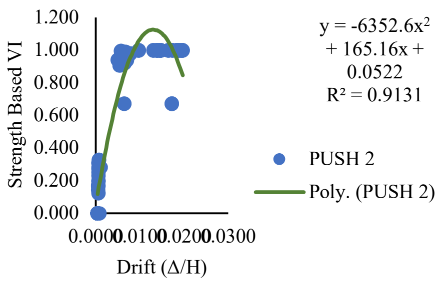

(xxix) Strength Based VI Group – 05

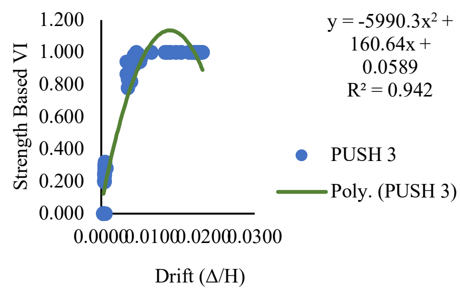

(xxx) Strength Based VI Group – 05

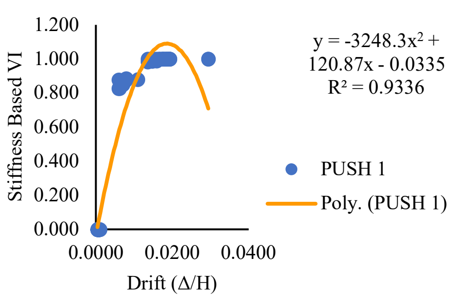

(xxxi) Stiffness Based VI Group – 01

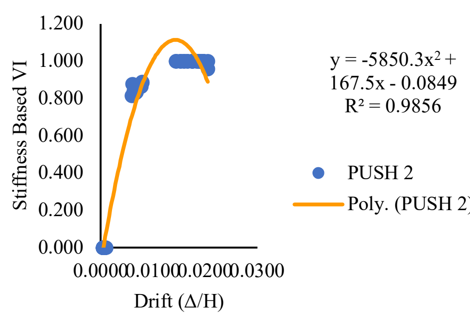

(xxxii) Stiffness Based VI Group – 01

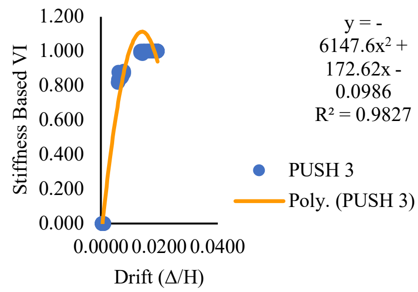

(xxxiv) Stiffness Based VI Group – 01

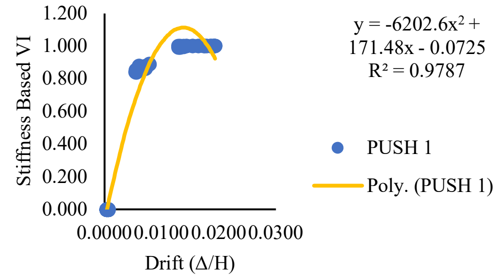

(xxxv) Stiffness Based VI Group – 02

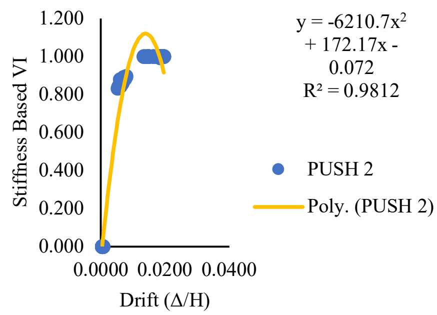

(xxxvi) Stiffness Based VI Group – 02

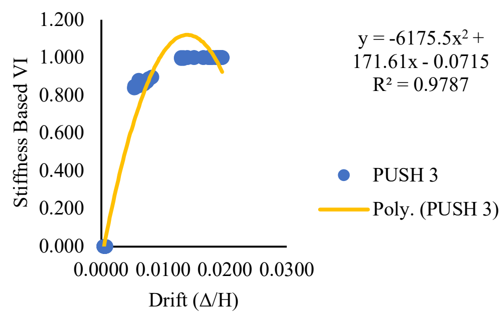

(xxxvii) Stiffness Based VI Group – 02

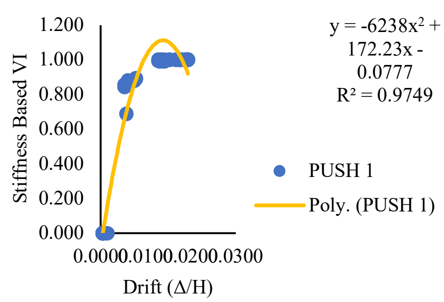

(xxxviii) Stiffness Based VI Group – 03

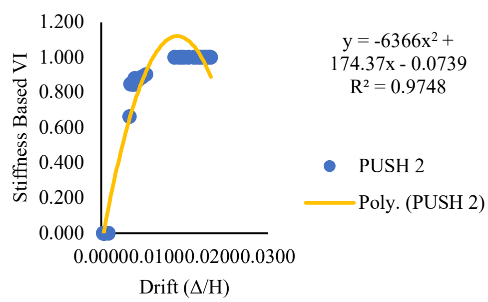

(xxxix) Stiffness Based VI Group – 03

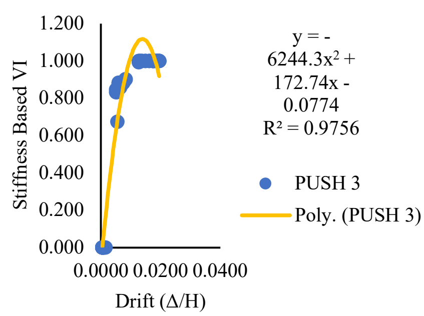

(xl) Stiffness Based VI Group – 03

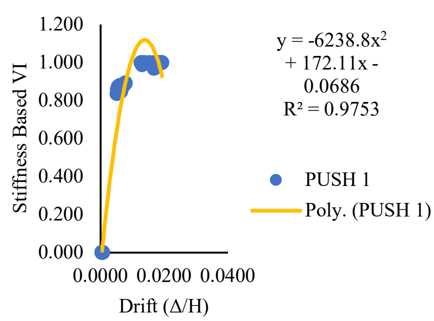

(xli) Stiffness Based VI Group – 04

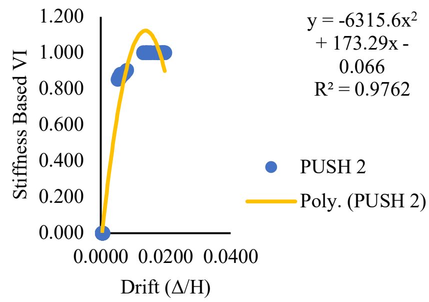

(xlii) Stiffness Based VI Group – 04

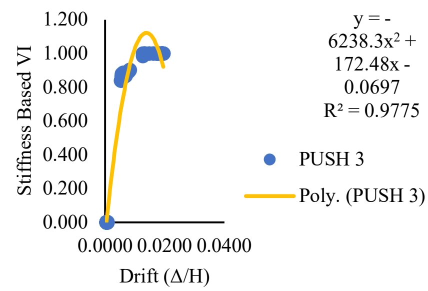

(xliii) Stiffness Based VI Group – 04

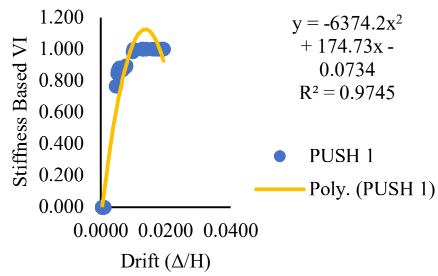

(xliv) Stiffness Based VI Group – 05

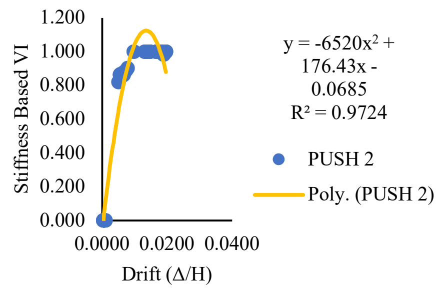

(xlv) Stiffness Based VI Group – 05

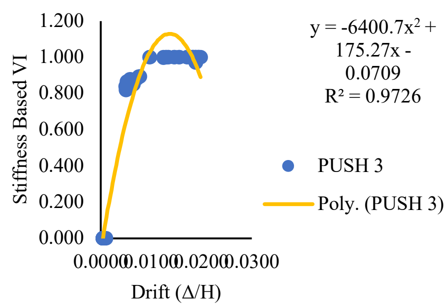

(xlvi) Stiffness Based VI Group – 05

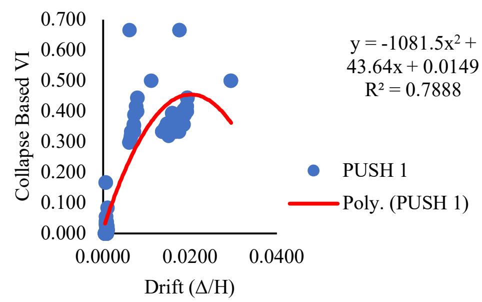

(xlvii) Collapse Based VI Group – 01

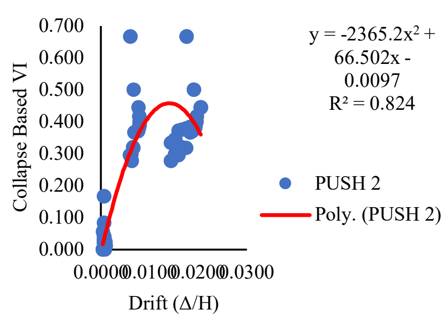

(xlviii) Collapse Based VI Group – 01

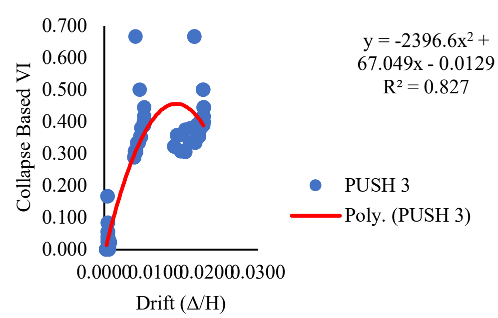

(xlix) Collapse Based VI Group – 01

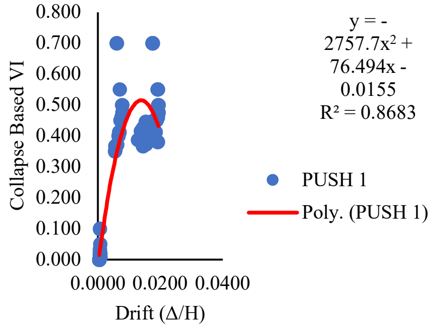

(l) Collapse Based VI Group – 02

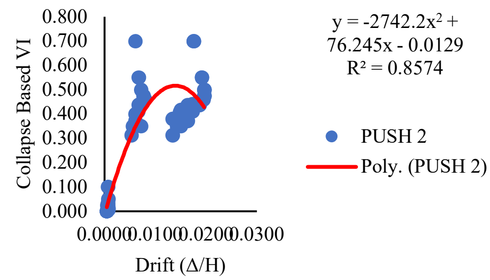

(li) Collapse Based VI Group – 02

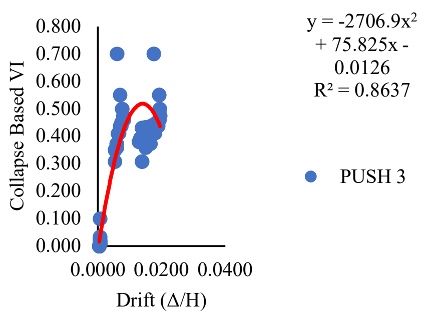

(lii) Collapse Based VI Group – 02

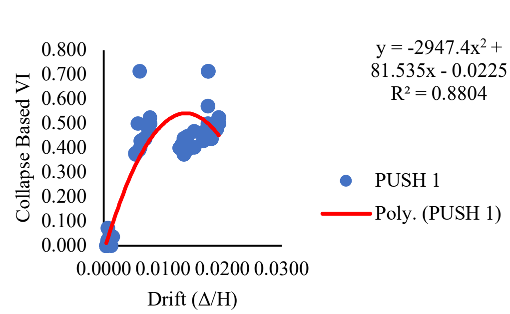

(liii) Collapse Based VI Group – 03

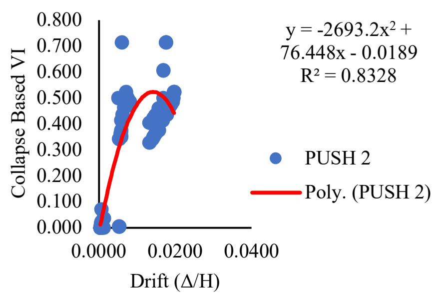

(liv) Collapse Based VI Group – 03

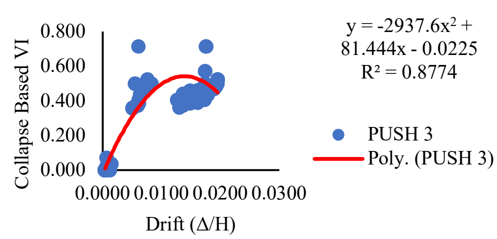

(lv) Collapse Based VI Group – 03

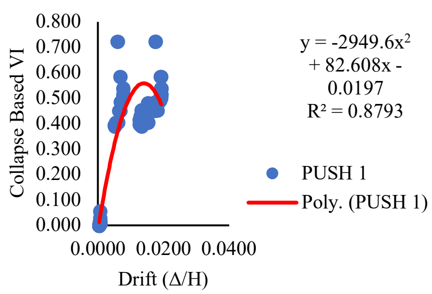

(lvi) Collapse Based VI Group – 04

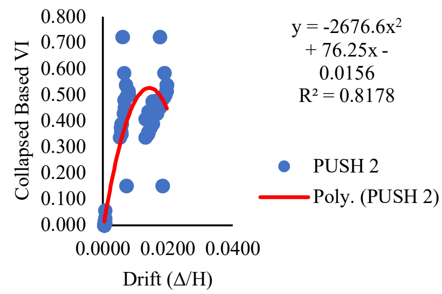

(lvii) Collapse Based VI Group – 04

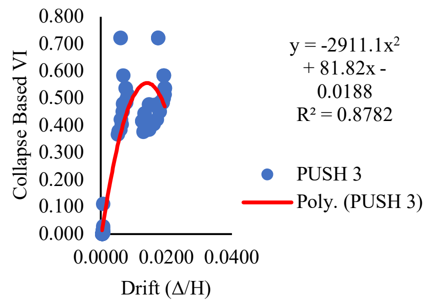

(lviii) Collapse Based VI Group – 04

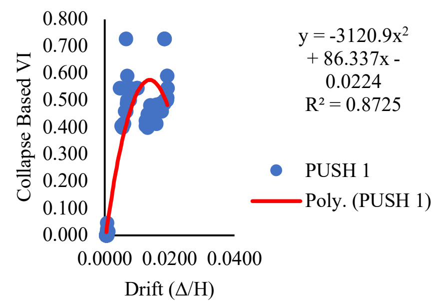

(lix) Collapse Based VI Group – 05

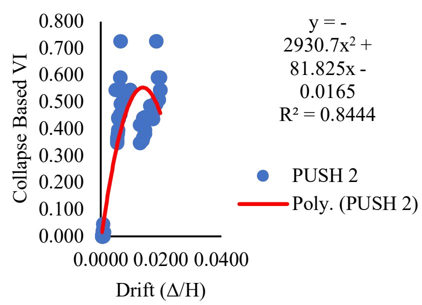

(lx) Collapse Based VI Group – 05

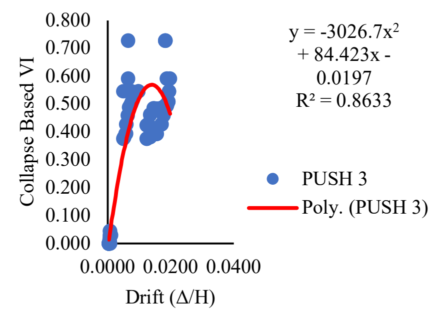

(lxi) Collapse Based VI Group – 05

Fig. 8: Shows the damage spectrum group of RCMRFs in respect to defines VI's

Conclusions

Many studies have been conducted in the past to comprehend performance evaluation methods. It is widely known that these evaluation methods can optimize nonlinear behavior by aligning applied demands (lateral loads) with structural capacity (internal resistance), but they are unable to convey the numerical scale of damage. Additionally, when compared to one another, the numerical techniques used were found to be inconsistent. Since damage cannot be quantified, the state of knowledge has been limited to evaluating nonlinear responses. Tall buildings have become more prevalent in urban areas due to vertical expansion, and expert seismic designers are now concerned about the damage to these tall structures. The achievement of acceptable limit states addresses the findings of various performance evaluation methodologies. For various acceptable limit states, performance levels describe the state of structural component damage. Due diligence is not given because these performance levels are defined in terms of attaining drift limitations, which stakeholders do not grasp.

Any structure's drift is a measurement of its ductility defined by the strain, curvature, and rotation of its structural component. Minor fractures initially emerge during seismic stress, which is followed by significant cracks or collapse as the ductility requirement rises. To track these ductility demands, drift-based VI have been proposed in the current study. The accomplishment of various performance levels during inelastic demand is defined using the drift-based VI's numerical scale. It is primarily a measurement of structural component cracking or spalling and can be used to estimate repairs and maintenance costs.

Loss of strength is a measurement of the decline in the structural element's resistive strength. When a structure's structural and non-structural components begin to deteriorate, large fissures can form when it is subjected to seismic load. The Strength-based VI that has been presented is a numerical scale that measures damage that a structure's system can withstand and may be connected to lost functionality (down-time).

Loss of rigidity signals the beginning of the deterioration of structural elements or the whole structure. Loss of stiffness is a sign that the building is about to give way and will no longer be safe for habitation. The proposed Stiffness-based VI can quantify this loss statistically and may be connected to the number of casualties.

A mechanism's subsequent transition of plastic hinges from one performance level to another shows a cumulative loss in ductility, strength, and stiffness. The suggested collapse-based VI can quantify these damages, including the need for repairs, downtime, and casualties.

For all 75 example RCMRFs, the proposed damage indices have been evaluated. The evaluation of VI's for a collection of RCMRFs offers a logical way to calculate the associated damage on a scale from zero to one. This relationship can be used to determine damage in any displacement situation. The suggested VI's are a possible technique for integrating the process of performance evaluation with that of damage assessment. The unique damage quantification approach that has been offered enables stakeholders to comprehend how well a building performs in terms of repairs, downtime, and causalities.

Acknowledgement

The authors of this work acknowledge the research contributions provided by all the referenced sources as well as the support of the Chairman of Kalinga University in New Raipur, Chhattisgarh, India, and the MGM College of Engineering in Nanded, India.

References

[1] Zameeruddin, M., Sangle, K.K., (2017a). Seismic Performance Evaluation of Reinforced Concrete Frames Subjected to Seismic Loads. Journal of Institute of Engineers, India Series A, DOI 10.1007/s40030-017-0196-0

[2] Zameeruddin, M., Sangle, K.K., (2016). Review of Recent Developments in the Performance-based Seismic Design of Reinforced Concrete Structures. Structure 6: 119-133. http://dx.doi.org/10.1016/j.istruc.2016.03.001

[3] Murty, C.V.R., Goswami R., Vijaynarayan A. R., Mehta V.V.,(2012). Some Concepts in Earthquake Behaviour of Buildings, Gujarat State Disaster Management Authority, Government of Gujarat, India.

[4] Azhdary, F., Shabakty, N., (2014). Performance based Design and Damages Estimation of Steel Frames with Consideration of Uncertainties. Technical Gazette, 21, 351–358. UDC/UDK 624.014.2.042.7:620.191.3

[5] Borg, R.C., Rossetto, T., (2010). Performance based Seismic Design and Assessment Methodologies: relation to Damage and Requirements. 8th Fib PhD Symposium in Kgs, Lyngby, Denmark

[6] Zameeruddin M and Sangle KK (2021a). Damage Assessment of Reinforced Concrete Moment Resisting using Performance-based Seismic Evaluation Procedure. Journal of King Saud University-Engineering Sciences, 33(4):1-13. https://doi.org/10.1016/j.jksues.2020.04.010

[7] ATC-40, Seismic evaluation and retrofit of existing concrete buildings. Redwood City (CA): Applied technical council, 1996.

[8] FEMA 273, NEHRP guidelines for the seismic rehabilitation of buildings. Washington (DC): Federal emergency management agency, 1996

[9] FEMA 356. Prestandard and commentary for the seismic rehabilitation of buildings. Washington (DC): Federal emergency management agency, 2000.

[10] Korkmaz, K. A., Irtem, E.,(2008) Evaluation of previous and current performance-based analysis method. The 14th World conference on earthquake engineering, Beijing, China. http://www.iitk.ac.in/nicee/wcee/article/14_14-0046.PDF.

[11] Boroujeni, A. R. K., (2013). Evaluation of various methods of FEMA 356 compare to FEMA 440. Journal of civil engineering and construction technology, 4(2); 51-55. DOI: 10.5897/JCECT12.082

[12] Chopra, A. K., Goel, R. K., (2000). Evaluation of NSP to estimate seismic deformation: SDF system. J. Struct. Eng., 126 (4); 482–490. DOI:10.1061/(ASCE)0733-9445(2000)126:4(482)

[13] ASCE/SEI 41. American society of civil engineers. Seismic rehabilitation of existing building. Reston, Virginia, 2007.

[14] Wilson EL, Habibullah A., (2000). SAP 2000/NL-PUSH software, Computer and structures, Inc (CSI), version 17.0, Berkely (CA. USA)

[15] BIS IS 456, Indian standard plain and reinforced concrete-code of practice (fourth revision). Bureau of Indian Standards, 2000, New Delhi.

[16] BIS IS 1786, Indian Standard for high strength deformed steel bars and wires for concrete reinforcement. Bureau of Indian Standards, 2008, New Delhi.

[17] BIS IS 1893, Indian Standard criteria for earthquake resistant design of structures (part 1): general provisions and buildings (fifth revision). Bureau of Indian Standards, 2002, New Delhi.

[18] BIS IS 13920. Indian Standard ductile detailing of reinforced concrete structures subjected to seismic forces– code of practice (incorporating amendment nos. 1 and 2). Bureau of Indian Standards, 2000–03, New Delhi.

[19] FEMA 445, 2006. Next-generation performance-based seismic design guideline program for new and existing buildings. Federal Emergency Management Agency, Washington (DC).

[20] Zameeruddin, M., Sangle, K.K., (2017b). Seismic damage assessment of reinforced concrete structure using nonlinear static analyses. KSCE J. Civil Eng. 21 (4), 1319–1330. https://doi.org/10.1007/s12205-016-0541-2.

[21] Zameeruddin, M., Sangle, K.K., (2017c). Energy-based damage assessment of RCMRFs using pushover. Asian J. Civil Eng. (BHRC) 18 (7), 1077–1093.

[22] Ghobarah, A., (2001). Performance-based design in earthquake engineering: state of development. Engineering Structures, 23, pp. 878–884.
DOI: 10.1016/S0141-0296(01)00036-0

[23] Mondal A., Ghosh S., Reddy G.R., (2013). Performance-based evaluation response reduction factor for ductile RC frames. Engineering Structures, 56. Pp 1808-1819.

[24] Ghosh, S., Datta, D., Katakdhond, A.A., (2011). Estimation of the Park–Ang damage index for planar multi-storey frames using equivalent single-degree systems. Engineering Structures, 33, 2509–2524.

[25] Inel, M., and Ozmen, H.B., (2006). Effects of plastic hinge properties in nonlinear analysis of reinforced concrete buildings. Engineering Structures, 28, 1494–1502.

[26] Lagaros, N.D., Fragiadakis, M., (2011). Evaluation of ASCE-41, ATC-40 and N2 static Pushover methods based on optimally designed buildings. Soil Dynamics and Earthquake Engineering, 31, 77–90.

[27] Sasaki, K.K., Freemanand, S.A., Paret, T.F., Multi-Mode Pushover Procedure (MMP) – A method to identify the effects of higher modes in a Pushover Analysis. 6th U.S. National Conference on Earthquake Engineering.

[28] Bo-quan LIU, Ming LIU, Ying-bin LI, (2004). Research & development of Performance-Based Seismic Design Theory. 13th World Conference on Earthquake Engineering Vancouver, B.C., Canada, Paper No. 2457

[29] Fajfar, P., (1999). Capacity Spectrum Method Based on Inelastic Demand Spectra. Earthquake Engineerin and Structral Dynamics, 28, 979-993

[30] Hirekhan, A., Zameeruddin, M., Charpe, P.S., (2023). Seismic Performance Evaluation of Indian code-designed Concrete Moment Resisting Frames using PBSE Procedures, European Chemical Bulletin, Volume 12(Special Issue 4), 7001-7024.

[31] Emrah Erduran and Ahmet Yakut (2007). Vulnerability Assessment of Reinforced Concrete Moment Resisting Frame Buildings. Journal of structural engineering, 133: 576-586. DOI: 10.1061/(ASCE)0733-9445(2007)133:4(576)